A Micro Approach to Quantitative Dehydration Sensor Development

by

Cobus Visser

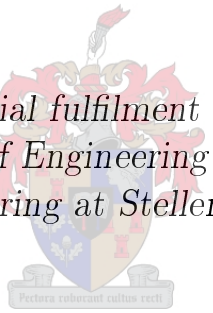

Thesis presented in partial fulfilment of the requirements for the degree of Master of Engineering (Mechatronic) in the Faculty of Engineering at Stellenbosch University

Supervisor: Prof. C. Scheffer

March 2015

Declaration

By submitting this thesis electronically, I declare that the entirety of the work contained therein is my own, original work, that I am the sole author thereof (save to the extent explicitly otherwise stated), that reproduction and publication thereof by Stellenbosch University will not infringe any third party rights and that I have not previously in its entirety or in part submitted it for obtaining any qualification.

Date: 2014/12/10 .....

Abstract

The assessment of dehydration is an ever elusive golden standard, even given the plethora of hydration markers that exist to date. Many literature sources acknowledge the need for a portable device that can be used as an indicative tool for hydration. This project sought to find a solution for assessing dehydration on a micro level looking for an indication of hydration by investigating the levels of water concentration in the skin and water compartments of the body using bioelectrical impedance, stratum corneum impedance and infrared spectrometry. Two studies were conducted to evaluate the efficacy of these devices: an infield study to assess the efficacy of the devices for measuring dehydration brought on by exercise in adults and an infant study where the devices where used to assess its ability to measure dehydration in infants who have succumbed to diarrhoea. The studies showed that the devices are not applicable in measuring real time hydration in exercising subjects as sweat was a perturbing factor in the measurements. The infant study provided promising results with regards to the usage of the infrared device. It is believed that these results could spur further investigation into the field of using infrared spectrometry as a dehydration marker. Dehydration still remains to be an ever elusive standard but the importance of finding a solution to quantitatively assess hydration is a field which could benefit the general population and its importance should not be underestimated.

Uittreksel

Die assessering van dehidrasie is steeds 'n ontwykende goue standaard selfs gegewe die oorvloed van hidrasiemerkers wat bestaan tot op datum. Baie literatuurbronne erken egter die behoefte aan 'n draagbare toestel wat as 'n hulpmiddel kan dien vir die evaluering van die vlakke van dehidrasie. Hierdie projek streef daarna om ondersoek in te stel tot die assessering van dehidrasie op 'n mikrovlak deur die waterkonsentrasies te meet in die vel en die verskeie waterkompartemente in die liggaam via die gebruik van bio-elektriese impedansie analise, stratum corneum impedansie analise en infrarooi-spektrometrie. Twee studies is gedoen om die doeltreffendheid van die toestelle te evalueer: 'n inveldstudie wat die hidrasievlakke van volwassenes meet wat ly aan dehidrasie weens oefening en 'n studie wat dehidrasie meet in neonate wat ly aan dehidrasie weens diarree. Die studies het bewyse gelewer dat die toestelle nie effektief is met betrekking tot die meet van dehidrasie in aktiewe volwassenes nie, weens die rede dat sweet 'n verstorende faktor is. Die neonate studie het belowende resultate verskaf met betrekking tot die gebruik van die infrarooi toestel. Daar word geglo dat hierdie resultate verdere ondersoek in die veld met betrekking tot infrarooi spektrometrie as 'n hidrasie merker kan motiveer. Finale bevindinge wys dat die kwantifisering van dehidrasie steeds 'n ontwykende standaard is, maar die belangrikheid van 'n moontlike oplossing sal voordelig wees vir die wêreld se volke en moet dus nie onderskat word nie.

Acknowledgements

I would like to express my sincerest gratitude to those who made this project possible. Thanks goes to Philips for funding the project and giving unequalled advice helping improve myself as a researcher. I thank Prof. C. Scheffer (Phd Eng.), Dr. Blackenberg (Phd Eng.) and Prof. J. Smith (Neonatologist) for their help in the planning and execution of the project. I would also like to thank the third party bodies who have given advice with regards to the project. These bodies include the lecturers from both the electrical and electronics and mechatronics departments of the engineering faculty of the University of Stellenbosch. Special thanks are given to SUSPI Gym and Tygerberg Hospital's G-ward for their support and helpfulness with the adult and infant studies.

I would also like to thank BERG offices for their everlasting support by helping and motivating me to carry on when times were dire. I am grateful for the experience and time that was given to me by the occupants of BERG and was it not for their help I would have faltered and would have ultimately failed.

Lastly, let it be known that in one's struggle and frustration one will become discouraged and will doubt his abilities and his confidence will surely diminish. In struggle depression will find you and hopefully there will be someone that will catch you and assure you that everything will be all right. I will never forget nor shall it be told to me otherwise the support and strength given to me by my family and friends. To my mother and father: my deepest and sincerest thanks for never letting me fall and always being there to catch me.

Nomenclature

C_C	The capacitance of the device's coaxial cable
f	Sampled signal frequency
f	Signal frequency
f_s	Sampling frequency
j	Imaginary number j
k	Frequency component of X_k
N	Total number of samples
n	Sample of x_n
R_R	The resistance used to limit the current and as a reference resistance for the voltage division between itself and Z_B
x_1	Voltage over the reference resistor (R_R) and the tissue impedance (Z_B)
x_2	Voltage over the impedance Z_B
X_k	Fourier transform of the signal x_n
x_n	Sampled signal
Z_B	The impedance of the measured tissue
ADC	Analog to Digital Converter
BIA	Bioelectrical Impedance Analysis
DDS	Direct Digital Synthesizer
ECF	Extracellular Fluid
ECG	Electrocardiograph
GUI	Graphical User Interface

IC Integrated circuit

ICF Intracellular Fluid

kSPS kilosamples per second

LED Light-Emitting Diode

MSPS Megasamples per second

PCB Printed Circuit Board

SC Stratum Corneum

TBW Total Body Water

TEWL Transepidermal Water Loss

Contents

Declaration i

Abstract ii

Uittreksel iii

Acknowledgements iv

Contents vii

List of Figures x

List of Tables xii

1 Introduction 1
- 1.1 Motivation . . . 1
- 1.2 Background . . . 1
- 1.3 Project Overview . . . 2
- 1.4 Objectives . . . 3

2 Literature Study 4
- 2.1 States of Dehydration . . . 4
  - 2.1.1 Hypertonic Hypovolemia . . . 4
  - 2.1.2 Isotonic Hypovolemia . . . 5
- 2.2 Markers of Dehydration . . . 5
- 2.3 Bioelectrical Impedance Analysis (BIA) . . . 7
  - 2.3.1 Single Frequency BIA (SF-BIA) . . . 9
  - 2.3.2 Multi-Frequency BIA (MF-BIA) . . . 9
  - 2.3.3 Bioelectrical Impedance Spectrometry (BIS) . . . 9
  - 2.3.4 Bioelectrical Impedance Vector Analysis (BIVA) . . . 9
  - 2.3.5 BIA as a Hydration Marker . . . 10
- 2.4 Stratum Corneum Hydration Probe . . . 11
  - 2.4.1 Electrical Probe . . . 11
  - 2.4.2 Fibre-Optic Refractometer . . . 12
  - 2.4.3 Electrical Characteristics of the Stratum Corneum . . . 12

2.5 Infrared Spectrometry . . . 13
2.5.1 Theory . . . 14
2.5.2 Skin . . . 15
2.6 Hypothesis . . . 18
2.7 Chapter Summary . . . 19

3 Device Design and Implementation 20
3.1 Device Descriptions . . . 20
3.1.1 BIA . . . 20
3.1.2 SC Analysis . . . 20
3.1.3 Infrared Spectrometry . . . 21
3.2 Circuit Design . . . 22
3.2.1 BIA and SC Impedance . . . 22
3.2.2 Infrared Spectrometry Circuit . . . 23
3.3 Voltage Supply . . . 26
3.4 Digital Interface . . . 26
3.4.1 Microcontroller . . . 27
3.4.2 Direct Digital Signal Synthesizer (DDS) . . . 28
3.4.3 WIFI Module . . . 28
3.5 Analogue and Digital Interconnectivity . . . 28
3.6 User Interface . . . 29
3.7 Chapter Summary . . . 32

4 Signal Processing 33
4.1 Discrete Fourier Analysis . . . 33
4.2 Signal Phase Calibration . . . 35
4.3 Circuit Calibration . . . 36
4.3.1 Cable Capacitance . . . 36
4.3.2 Amplifier Calibration . . . 37
4.3.3 Impedance Calculating Algorithm . . . 38
4.3.4 Sampling Frequency Shifting Algorithm . . . 39
4.4 Chapter Summary . . . 39

5 Observations 41
5.1 Impedance Accuracy and Validation . . . 41
5.2 BIA Observation . . . 42
5.3 SC Observation . . . 42
5.4 IR Spectrometry Observation . . . 43
5.5 Chapter Summary . . . 45

6 Testing Methodology and Results 46
6.1 Standardized Testing and Validation Procedure . . . 46
6.1.1 Ethical Approval . . . 46
6.1.2 Adult Study . . . 47

6.1.3 Infant Study 48
6.2 Results 50
6.2.1 Data Preparation 50
6.2.2 BIA Adult Results 51
6.2.3 SC Adult Results 52
6.2.4 IR Adult Results 52
6.2.5 Adult Discussion 53
6.2.6 Plasma Osmolality 56
6.2.7 Infrared Spectrometry Infant 57
6.2.8 Infrared Spectrometry Infant: Discussion 58
6.2.9 Stratum Corneum Infant 59
6.2.10 Stratum Corneum Infant: Discussion 60
6.3 Chapter Summary 60

7 Conclusion and Future Work **61**
7.1 Conclusion 61
7.2 Future Work 62
7.2.1 Hardware and Design 62
7.2.1.1 Microprocessor 62
7.2.1.2 Sampling Methods 63
7.2.1.3 Digital Interface 63
7.2.1.4 WIFI 63
7.2.1.5 Infrared Spectrometry 64
7.2.2 Research 64

Appendices **65**

A Printed Circuit Boards **66**

B Monte Carlo Simulation **69**

C Ethical Approval **72**

D Letter of Consent **76**

E Datasheets **86**

List of References **93**

List of Figures

2.1 Equivalent circuit model for the human body 7
2.2 Cole-Cole Plot 8
2.3 BIVA Example 10
2.4 Workings of the Fiber-Optic Refractometer [1] 13
2.5 Optical and Electrical Probe [1] 13
2.6 Examples of possible stratum corneum measuring devices 13
2.7 Layers of skin: epidermis, dermis and subcutaneous tissue [2]. . . . 17
2.8 Optical absorption coefficient of deoxyhaemoglobin, oxyhaemoglobin, water and lipids [3] 18

3.1 Stratum corneum probe encapsulated in silicon with coaxial cable attached 21
3.2 Infrared probe concealed in silicon 22
3.3 BIA and SC circuit configuration 24
3.4 IR and LED circuit configuration 26
3.5 Voltage splitter and regulator 27
3.6 Overview diagram of digital setup 29
3.7 User interfaced programmed with Qt Creator 30

4.1 Sequential sampling of an arbitrary analogue signal to produce the signals x_1 and x_2 36
4.2 Algorithm implemented by the microcontroller to calculate the body impedance 38
4.3 Flow diagram depicting frequency shifting to accommodate limited microcontroller memory 40

5.1 Magnitude and phase measurements of a parallel resistor and capacitance circuit 41
5.2 BIA ankle to ankle measurements on a single subject 43
5.3 SC impedance results from hydration test performed on the stratum corneum for 1 minute and 5 minutes of exposure to water vapour . 44
5.4 Infrared hydration test performed on the stratum corneum for 1 minute and 5 minutes of exposure to water vapour 44

6.1 Adult testing protocol: Phase 1 and Phase 2 49

6.2 Grouped BIA results 51
6.3 Implementation of the BIA device. 51
6.4 Grouped stratum corneum results 52
6.5 Implementation of the SC device. 53
6.6 Grouped adult infrared results 53
6.7 Adult grouped measurements shown as IR (1300 nm:1480 nm) ratio 54
6.8 Implementation of the IR spectrometry device. 54
6.9 Plasma osmolality analysis from the adult study 56
6.10 Infrared spectrometry observations of four infant subjects 58
6.11 Illustrated implementation of the SC and IR spectrometry devices on an infant. 59
6.12 Grouped infant stratum corneum results 60

A.1 Stratum corneum circuit configuration 66
A.2 Top and bottom layer of IR pcb circuitry 67
A.3 Rail splitter, amplifier, buffer and DDS pcb top layer 67
A.4 Rail splitter, amplifier, buffer and DDS pcb bottom layer 68

B.1 Fluence rate observed in a homogeneous semi-infinite medium subjected to a point source of 1300 nm of IR light 70
B.2 Fluence rate observed in a homogeneous semi-infinite medium subjected to a point source of 1480 nm of IR light 70
B.3 Fluence rate observed at the boundary of the air and medium subjected to 1300 nm and 1480 nm of IR light 71

List of Tables

6.1 Linear regression analysis of the measured variables: BIA, SC and IR 55
6.2 Linear regression analysis of BIA, SC and IR variables with regards to plasma osmolality 57

Chapter 1

Introduction

1.1 Motivation

Dehydration can be experienced by all ages though it has been found to have a larger detrimental effect on children [4, 5]. Dehydration mostly found with children, under the age of four, is brought on by vomiting or diarrhoea [5]. It is mentioned that diarrhoea is the "second leading deadly killer" in children under the age of five [6]. So much as one out of five children die as a result of dehydration, weakened immunity and malnutrition associated with diarrhoea in the world [6]. It is also estimated that 1,5 million children die due to diarrhoea each year [6]. To prevent one of the key factors of this mortality rate, dehydration, it is obvious that oral rehydration needs to take place, but when this should take place is uncertain as the general populous do not know how to asses an infants' dehydration state given the physiological symptoms thereof. This shows the need for an easy to use device that can assess the hydration status of infants and young children and can be operated by the general populous.

1.2 Background

Hydration is a complex and misunderstood state which to date have eluded several attempts at being quantitatively defined. Even the state of euhydration (normal hydration) is an oscillating and ever dynamic occurrence [7]. Many literature sources claim that there is no golden standard in assessing dehydration even with the several markers that exist to date. Though some of these markers do assess dehydration to a certain accuracy its ability is hindered by the fact that it is either costly, non-portable and more suited for technicians with some expertise in the field. Most probably the greatest disadvantage of reliable hydration markers is its ineptitude to do infield measurements as they require some form of standardised setting (e.g. consuming isotope solution, blood analysis etc.).

1.3 Project Overview

In this project it is sought to find an inexpensive method to assess dehydration for underserved settlements. It is believed that underserved settlements, due to their lack of basic services, would be more prone to dehydration brought on by diarrhoea. It is also assumed that the lack of education could indirectly contribute to the misidentification of dehydration. In addition to catering to the hydration assessment of infants it is also strived to find a way as to asses dehydration in adults as it is believed that there exists a market with regards to assessing dehydration brought on by endurance sport.

Three methods were chosen to asses dehydration namely ankle to ankle Bioelectrical Impedance Analysis (BIA), Stratum Corneum(SC) Impedance analysis and Infrared (IR) Spectrometry. These methods were chosen due to a lack of literature with regards to their efficacy as dehydration markers. Bioelectrical analysis though widely known has only been found by one literature source to be useful as an hydration marker. Essentially BIA can be used to derive total body water, however this is under euhydrated circumstances. The stratum corneum approach is demonstrated by several literature sources to be a tool for assessing skin hydration [1, 8, 9]. In this project it is used to assess the possible change in transepidermal water loss (TEWL) brought on by dehydration. Infrared spectrometry is a field that piqued interest in the project as no sources were found on its efficacy as a hydration marker less so as an in vivo instrument. The closest source with regards to IR spectrometry in measuring hydration is by Nachabé et al. [3] where they used IR spectroscopy as a method to determine the concentration of lipids and water given the mixed medium. This was however done in vitro. It is hoped that with the culmination of the BIA, SC analysis and IR spectrometry devices that a solution to the elusive golden standard can be found.

Certain observations were made with the three devices which tested their validity in its ability to measure levels of hydration. The IR spectrometry and SC impedance analysis devices showed promise as the obtained results coincided with the theory. The devices were tested using a method inspired by the sorption-desorption test. The skin was subjected to water vapour for a set amount of time enabling the stratum corneum to absorb the water. This was done for 1 minute and then 5 minutes with measurements in between. The IR device and SC impedance devices were able to measure the difference between the dry skin, the 1 minute exposed to water vapour skin and the 5 minute exposed to water vapour skin. The validation method used for the BIA device was to take several measurements of a subject. The measurements were then used to see if the required Cole-Cole plot could be found. Alas this was not the case and it was assumed that the BIA device's current was too low to penetrate into deeper tissue. The BIA device was not omitted from the study because it was postulated that the device was measuring the skin layers of the tissue and it was believed that this could still be used as an indication

of dehydration.

Two studies were conducted with the three devices, namely an adult study and an infant study. The adult test comprised of 9 adults who were subjected to strenuous exercise to induce hypertonic hypovolemia. Subjects had to complete three exercise sessions per day for three days with measurements being taken between each session. The results from this study were contradictory to the theory and it was believed measurements were perturbed by the accumulation of sweat in the skin. The study proved that the project's devices were not suited for infield measurements with regards to measuring hydration in active people. The infant test was conducted in Tygerberg hospital where infants would be measured that has succumbed to gastrointestinal distress leading to isotonic hypovolemia. Unfortunately the number of subjects was few as the ethical application was approved close to the deadline of the project. However of the four measured subjects IR spectrometry shows promise and should not be ignored due to the small number of subjects. It is believed that infrared spectrometry has the ability to measure hydration levels in the skin leading to an assessment of overall hydration.

This document strives to explain the processes which were used to manufacture three different devices. It will discuss the theory behind each device and how it can be implemented as a dehydration marker. Signal analysis, circuit design, microcontroller and computer programming, simulation and statistical methods were implemented to fabricate, validate and test these devices.

1.4 Objectives

- Develop three sensors that can be used as hydration markers, namely the BIA device, stratum corneum impedance probe and the IR spectrometry device.
- Ensure the devices are non-invasive and safe to use with both infants and adults.
- Incorporate technologies that will ensure the device to become portable in the final design for commercial use.
- Incorporate technologies that are inexpensive as to cater for underserved communities.
- Test and validate the devices with both adults and infants.
- Deliver a proof of concept and efficacy for the above-mentioned devices.
- Attempt to produce a golden standard for dehydration by combining the different devices.

Chapter 2

Literature Study

2.1 States of Dehydration

Though hydration is a well known term it is highly misinterpreted as just a state of water surplus or deficit in the body. However this is not the case as the state of dehydration can be classified into two states, namely: hypertonic hypovolemia and isotonic hypovolemia (frequently shortened to hypovolemia)[10]. These states of dehydration are investigated as these states determine which physiological mechanisms are involved in the regulation of homeostasis in the body.

2.1.1 Hypertonic Hypovolemia

This state of dehydration is well known to most people as this is the most common dehydration one would experience from excessive sweating brought on by exercise [11]. Other factors that cause this type of dehydration is sweat loss due to environmental heat stress and fever, inadequate fluid intake and osmotic diarrhoea [10, 11]. Hypertonic hypovolemia describes the state where water loss occurs faster than solute loss via the processes as previously described [10, 11]. This causes the plasma osmolality to increase resulting in a concentration gradient between intracellular fluid and extracellular fluid. This causes a water shift from the intracellular fluid to the extracellular fluid [10, 11]. If hypertonic hypovolemia should persist and plasma osmolality rises with 2% of its norm, osmoreseptors will trigger a hormonal response resulting in the release of arginine vasopressin (AVP) (also known as antidiuretic hormone (ADH)) [10, 12]. These hormones stimulate renal reabsorption in the kidneys where the water in the kidneys moves via osmosis from the tubules back into the bloodstream, normalising plasma osmolality [10, 12]. Other effects include the stimulation of the sensation related to thirst which motivates the body to consume water [12]. It should also be noted that the mentioned plasma osmolality threshold relates to approximately 2% loss of body mass due to isotonic hypervolemia water loss [10].

Some literature sources also describe how hyperosmolality can decrease heat dissipation responses in the body by influencing blood flow and and sweating [13]. This results in the body having a delayed vasodilation response in the face of dehydration and it has been mentioned how this decreases blood flow with dehydration in prolonged exercise [13].

2.1.2 Isotonic Hypovolemia

This state of dehydration is interesting, with the onset of isotonic loss of water and solute the plasma osmolality remains the same [10, 11]. This results in the osmoreseptors to not become stimulated even in the presence of dehydration. The regulatory device for such a case of dehydration is baroreceptors that become stimulated with the onset of a blood volume deficit [10]. This state of dehydration is fairly dangerous as its regulatory devices only become active when the body has lost approximately 4% of its mass due to water loss [10]. This relates to a difference in blood volume of approximately 10%. This means that the regulatory mechanism only becomes active in the case of severe dehydration. In the case where 10% loss in blood volume occurs baroreceptors will trigger a hormonal release of angiotensin resulting in the formation of angiotensin II [10, 12]. Angiotensin II stimulates the vasoconstriction of arterioles causing blood pressure to rise. Angiotensin II also stimulates the adrenal cortex which secretes aldosterone which in turn stimulates the reabsorption of salt and water from the kidneys [12]. Again, homeostasis is kept through the regulatory mechanism.

This state of dehydration is brought on by diarrhoea, vomiting and exposure to cold high altitude environmental.

2.2 Markers of Dehydration

With the states of dehydration now defined it is necessary to derive the method which will be used to measure and asses dehydration. Though there are a handful of different ways to asses dehydration a majority of literature suggests that there are no golden standard [7, 10]. These markers of dehydration include:

Isotope solution This marker is used to determine the total body water content of the body. This is done by orally ingesting a certain amount of deuterium oxide (D_2O) and waiting until the solution has equilibrated to the different water compartments in the body. This usually takes around three to four hours [14]. Blood, saliva, breast milk or urine samples are then used to find the concentration of deuterium therein. Assuming that deuterium oxide equilibrates similarly to water and distributes evenly among the water compartment in the body an approximate TBW content can be calculated. This method can measure within 1–2% accuracy of TBW [7, 14]. Even though this method is highly praised as a hydration

marker its potential is stunted by its high costs, its time consuming process, learning curve and poor portability makes it a poor hydration marker for real time and in field hydration assessment.

BIA Also a body composition assessment BIA calculates the extracellular fluid (ECF) and the intracellular fluid (ICW) of the body. Though primarily used to derive the body's composition through predefined equations given certain prerequisites (hydrated, physically healthy etc.) it has been shown by Röthlingshöfer et al. that BIA can be used to detect a change in the water compartments of the body [15]. Armstrong describes BIA as needing moderate technical expertise, being moderately costly and is to some extent portable [7].

Body mass Given if hydration is measured in a small window of time body mass would be the best option as a hydration assessor. The method is simple, all mass lost could be attributed to water loss be it through sweat, urine, respiratory losses etc. with the exception of excrement [7, 14]. This method however becomes a poor assessor when the window of observation stretches across days or months this being due to possible weight loss/gain and food intake [7]. This method still remains the main assessor for dehydration due to its simplicity and low cost [7].

Plasma osmolality This method is argued by some as being the closest to a standard for assessing dehydration [7]. In the event of acute hypotonic hypervolemic loss a person's blood solute will increase and thus lead to an increase in plasma osmolality [10, 11]. A blood sample is drawn from the person and the plasma osmolality will give an indication of dehydration. This method has a flaw worth noticing, literature has explained that a change in plasma osmolality will only occur when the dehydrated subject has lost more than 2–3% of their body mass due to dehydration [10, 14]. This method will thus only become useful at the point where the body has succumbed to moderate dehydration. This method requires technical expertise and is thus a costly and time consuming method. Again this will not be an effective hydration assessment method for in field measurements.

Urine Urine colour, osmolality, specific gravity and conductivity have all been used as markers for dehydration [7, 14]. Urine colour, though not a preferred method for assessment, is a good method for fast and immediate qualitative assessment. Whereas urine osmolality and conductivity requires analysis, which is a costly and time consuming process. Urine indices as a measure for dehydration are stunted due to the fact that it reacts slower to fluid intakes than that of plasma osmolality.

Saliva Similar to that of the urine assessment saliva requires analysis and is thus costly and time consuming [7].

The markers as mentioned above have been described by Armstrong as having a low likelihood in identifying dehydration with the exception of isotope dilution, which he rates as a possible high likelihood and plasma osmolality as having a moderate likelihood. The markers having a moderate to high likelihood are markers that requires some kind of analysis which is time consuming and costly and cannot be done by the general populous. One of the more detrimental disadvantages of these markers are that they are in no sense portable and cannot be used for infield and real time measurements. It can thus be said that there exists no marker that adheres to the objectives set out in Chapter 1.

All the markers mentioned in the previous section falls short in some or other way as a potential infield, inexpensive and accurate marker. However, if the costs regarding BIA could be lessened and be developed to be user-friendly it could proof to be a useful marker for dehydration. BIA will therefore be the only existing marker that will be considered in this study, all other devices will be new concepts. The following sections will propose different methods that could be used as hydration markers. Each section provides the theory behind each method and discusses why the method in question is a viable option for assessing dehydration.

2.3 Bioelectrical Impedance Analysis (BIA)

Bioelectrical impedance analysis is described by several authors as an electrical method that can accurately determine different compositions of the human body such as total body water (TBW), fat free mass (FFM), intracellular water (ICW) and extracellular water (ECW) [15, 16, 17]. This method measures the resistance of the ECW and ICW of the body. This method can be used for detecting the presence of alien tissue and disease and can be used as a diagnosis tool for assessing nutritional wellbeing and hydration status [15, 16, 17].

BIA works on the principle of measuring the resistances of the body and implementing the measurements in predefined sets of equations leading to an estimate of the body's TBW, FFM etc. Several papers use the parallel circuit model to approximate the electrical properties of the human body [15, 16, 17].

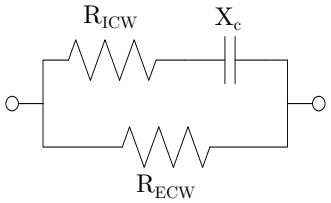

Figure 2.1: Equivalent circuit model for the human body

Figure 2.1 depicts the circuit approximation of the body where R_{ECW} is the resistance of the ECW of the body, R_{ICW} is the resistance of the ICW of the body and X_c is the capacitance reactance due to the cell membranes separating the ECW from the ICW [16, 17]. At low frequencies the capacitor would act like an almost perfect insulator and the total resistance would thus be the ECW resistance alone. At very high frequencies the capacitor will become an almost perfect conductor and the measured resistance will thus be the paralleled resistance of R_{ICW} and R_{ECW}. It is assumed that when a low frequency current is introduced to the body that the ECW will conduct the entirety of the current, whereas at high frequency it is believed that the current will pass through both the ECW, cell membrane and ICW [15]. The literature explains that measurements taken with the above-mentioned frequencies are not achievable and will most likely result in perturbed measurements [17]. The impedance can however be approximated using a Cole-Cole plot which can be produced over realizable frequencies.

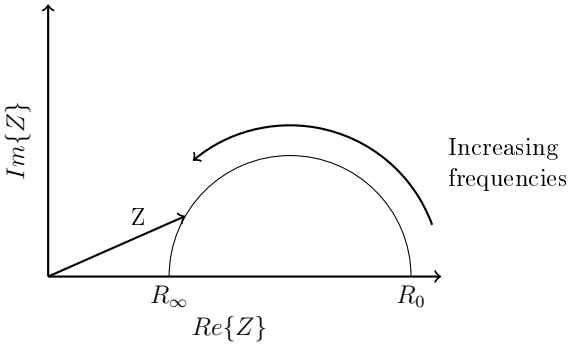

Figure 2.2: Cole-Cole Plot

The Cole-Cole plot is derived by measuring the impedance of the body at several frequencies and plotting the reactance of the body against the resistance of the body [15, 16, 17]. Several literature sources shows that the Cole-Cole plot can be produced in the frequency range of 5–1000 kHz and that it produces a circular distribution of impedances which is illustrated in Figure 2.2 [15, 16, 17]. As mentioned, measurements at high and low frequencies are not achievable. The Cole-Cole plot can however be extrapolated by the assumption that the varying impedances will form a semi-circle on the resistance axis with increasing frequencies [16, 17]. With the extrapolation of the Cole-Cole plot it is possible to find R_∞ and R_0. It can easily be seen that R_0 relates to the ECW of the body and R_∞ relates to ECW and ICW when referring to Figure 2.1. These measured resistances are used in several different predefined equations to calculate TBW, FFM etc.

There are several methods and equations to calculate the body's composition through bioelectrical impedance. The following sections present an overview of these methods.

2.3.1 Single Frequency BIA (SF-BIA)

Single frequency analysis is the measurement and implementation of the impedance of the body measured at 50 kHz [17, 18]. At this frequency it is believed that the measured impedance is mostly a result of the ECW resistivity and about 25% of ICW [17, 18]. SF-BIA results are based on mixture theories and empirical equations [17]. These theories and equations are derived from healthy subjects under standardized conditions. It is mentioned that SF-BIA does not give valid information if the subject in question is not in a state of euhydration [17]. SF-BIA has the ability to predict FFM and TBW in euhydrated subjects [17].

2.3.2 Multi-Frequency BIA (MF-BIA)

MF-BIA use impedance measurements at multiple frequencies together with empirical linear regression models to evaluate TBW, ICW, ECW and FFM [17, 18, 19]. It is mentioned that MF-BIA predicts ECW better than SF-BIA [17, 18]. It is also mentioned that MF-BIA predicts TBW more accurately than Bioelectrical Impedance Spectrometry (BIS) (mentioned in the next section) but not as accurately as SF-BIA.[17]

2.3.3 Bioelectrical Impedance Spectrometry (BIS)

Bioelectrical Impedance Spectrometry (BIS) like MF-BIA calculates the impedance over a range of different frequencies [19]. The difference lies in that BIS uses mathematical modelling (Cole-Cole plot) to calculate R_0 and R_∞ as mentioned above [17, 18, 19]. The results are then implemented in Hanai mixture equations to produce results related to TBW, FFM etc. [17, 18, 19]. This method is described as producing fairly accurate results in healthy subjects but becomes flawed when implemented on unhealthy or diseased subjects [17, 18].

2.3.4 Bioelectrical Impedance Vector Analysis (BIVA)

The methods mentioned above all rely on standardised equations. These equations were developed from various tests done on healthy subjects. It is because of this reason that the equations exhibit an error due to subjects who exhibit a condition that deviates from a standard and healthy physiological state. Several papers mentions this error in BIA due to subjects who exhibit dehydration, illness, disease etc [16, 17, 18]. In a case such as this one impedance as a standalone measurement can be used as a basis for measuring dehydration, nutritional status etc.

Bioelectrical Impedance Vector Analysis (BIVA)is a method that uses impedance as a standalone measurement for medical assessment. This method is

not dependant on equations for results and thus avoids errors brought on by standard equations [17]. The only affecting factor present is the measurements of variability in subject composition and impedance measurement error [17]. Figure 2.3, given below, is an example of a BIVA plot. As can be seen the axis of the plot is the reactance and resistance of the subject divided by the subject's height. The impedance measurement produces a point vector on the plot and this vector can fall within certain previously defined criteria which assesses a certain medical condition, for example dehydration. These criteria take the form of ellipses that indicates the tolerance of a certain healthy condition. The project will be aimed at producing these criteria for assessing the hydration status of people.

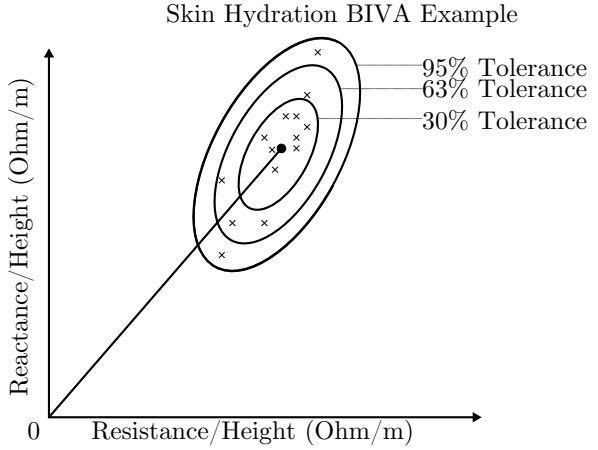

Figure 2.3: BIVA Example

2.3.5 BIA as a Hydration Marker

As mentioned above, several papers state that BIA impedance measurements are influenced by one's health and hydration status causing errors when using the appropriate standardised equations [16, 17]. It would thus be sensible to implement the BIVA as a hydration marker seeing that this method does not use any of the standardised equations and the different hydration criteria as shown in 2.3 can be derived through completing the project's studies. Additionally BIS can be used to extrapolate the resistances related to ECW and ICW through the use of the Cole-Cole plot.

Röthlingshöfer implemented various impedance measurements over various frequencies and found that a definite change in impedance is evident in subjects exhibiting dehydration [15]. More noticeably is that Röthlingshöfer believes that BIA can be used to measure and detect dehydration during physical exercise. This implies that a dynamic measuring sensor for dehydration could be possible.

2.4 Stratum Corneum Hydration Probe

The statum corneum is the outermost layer found on the skin [1, 8, 20]. This layer of dead lipid laden keratincytes, though only 15 µm thick, is responsible for protecting the hydrated tissue underneath [20]. More interestingly the stratum corneum is hygroscopic, meaning that it has the ability to absorb and retain water [1]. It is due to this characteristic of the stratum corneum which can make it a valuable hydration indicator. The stratum corneum, due to its hygroscopicity, can absorb transepidermal water loss (TEWL) [20]. The hydration measurement of the stratum corneum could thus give some indication to overall hydration and not just skin hydration which is the main focus of literature found on the subject. Unfortunately no literature could be found that explicitly states that the rate of transepidermal water loss is a measure of overall body hydration. However, it can be assumed that transepidermal water loss would decrease if a water deficit is present in the body. This can be a result of the body's attempt at preserving blood pressure via vasoconstriction upholding homeostasis in its attempt to avoid injury to vital internal organs by restricting water transport to less important parts of the body (for example skin) [4, 21]. In addition to this assumption several web-pages suggest that dry skin is a symptom of dehydration [21, 22]. From the last two statements enough motivation is given to investigate the stratum corneum's hydration as a marker of overall hydration.

Several sensors and methods exist that can assess hydration in the stratum corneum. These can range from devices implementing electrical, microwave and infrared spectroscopy [8]. It would seem that an electrical approach is more favourable seeing that several companies have developed electrical probes that can measure conductance and capacitance of the stratum corneum [8, 20]. Examples of these probes are the Corneometer, that uses capacitance as a measure for hydration, and the Skicon that uses conductance as a method for evaluating skin hydration [8]. The following sections describe two types of probes that was found to have some promise in measuring skin hydration .

2.4.1 Electrical Probe

It is mentioned in literature that the conductance and capacitance of the stratum corneum can give some indication to the skin's hydration state [8, 9, 20]. It is hoped that in doing so will give some indication about the state of hydration in the body. The most widely used measurement device is an electrical probe that will measure the change in skin hydration due to change in dielectric constant brought on by the water content in the stratum corneum. These probes consist of two electrodes which will deliver the current to the skin. In the case of measuring capacitance the electrodes will be covered in a known material which will act as a protective layer to the electrodes and as a way to prohibit galvanic contact [8]. Due to the last mentioned statement the elec-

trodes are isolated from the skin and the measurement cannot be influenced by salt or ion residues on the skin [8]. The stratum corneum will act as an added dielectric for the two electrodes forming a closed capacitor. An alternating current is implemented on the electrodes and the capacitance of the skin can thus be measured. A probe using conductance as a method for measuring has bare electrodes and contact with the skin is important to ensure accurate measurements [8].

Both methods have their advantages and disadvantages. It is mentioned that the measurements for capacitance can be disproportionately low compared with conductance and that capacitance is a less sensitive measurement for water content in the stratum corneum [20]. Hachiro et al. [20] argues that conductance gives a better correlation towards skin hydration assessment.

2.4.2 Fibre-Optic Refractometer

Takeo and Hattori presented a creative way of measuring the hydration state of the stratum corneum, using the change in refractive index due to its water content [1]. They incorporated a fibre-optic probe consisting of fibre-optic wires stripped bare over a u-shaped interface. When pressed against the skin the bare region of the fibre-optic is covered. When light travels through the wire it effectively reflects of the walls of the cladding. When the light approaches the region where the cladding is stripped off the light will either reflect at the boundary of the fibre-optic medium and the skin or the light will refract out of the fibre-optic into the skin. If the refractive index of the optic wire (n_{core}) is greater than that of the skin (n_{skin}) the majority of the light will reflect and the optical output will be high. In the case where n_{skin} is greater than n_{core} the majority of the light will refract and the optical output will be low. The optical output of the wire can thus be measured to acquire an indication of skin hydration.

2.4.3 Electrical Characteristics of the Stratum Corneum

For the purpose of this project it was chosen to follow the electrical probe approach. It is believed that more information is obtainable through impedance measurements seeing as it gives insight to the conductance and admittance of the stratum corneum itself. It was further decided that the impedance shall be measured over several frequencies as it has been mentioned that the impedance with regards to low frequencies relates predominantly to the stratum corneum. With higher frequencies it has been noted to be predominated by the deeper tissues [9]. It is mentioned by Birgersson that the electrical significance of the stratum corneum should not be ignored as it is not negligible even at the frequency of 1 MHz [23]. Further Birgersson argued that the stratum corneum will be the dominant impedance up to 100 kHz. Martinsen et al. [9] however approuched stratum corneum impedance dominance through

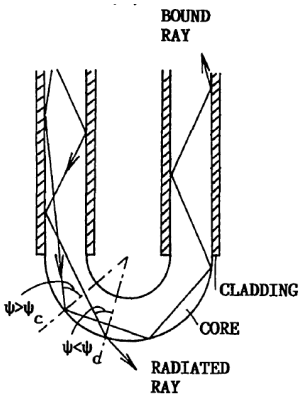

Figure 2.4: Workings of the Fiber-Optic Refractometer [1]

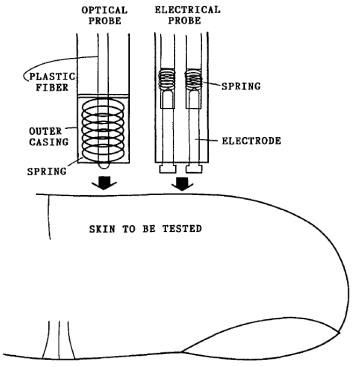

Figure 2.5: Optical and Electrical Probe [1]

Figure 2.6: Examples of possible stratum corneum measuring devices

mathematical modelling. They showed that the stratum corneum only dominated the frequency spectrum up to 1 kHz and that at 1 MHz the stratum corneum only exhibited 5% of the total measured impedance. Regardless of the true depth of measurement of the stratum corneum over the spectrum it was decided that the stratum corneum will still be measured over the entire available frequency spectrum possible by the project's devices. This was to investigate the electrical effects of dehydration on the stratum corneum and in the case of Martinsen's argument it could go so far as to give information with regards to deeper tissue hydration.

2.5 Infrared Spectrometry

Optical spectroscopy plays an important role in many diagnostic and therapeutic applications in medicine [24]. It is widely known as a diagnostic tool for monitoring blood oxydation, Doppler flowmetry, pulse oximetry, cancer through fluorescence etc. It has also been shown that it can be used as an analysis tool for serum, urine and saliva [25, 26]. Its uses are infinite and could prove to be an indispensable in vivo method for measuring dehydration.

Several papers argue that plasma osmolality is the most reliable marker for assessing dehydration [7, 27]. Unfortunately the general method for measuring plasma osmolality is through a freezing point depression method. For this measurement to be done blood has to be extracted from the subject. This is an invasive method and strongly comes in contrast with the objectives of this project. This spurred the investigation into diffuse optical spectrometry, seeing as this method is non-invasive and can be used in vivo. Diffuse spectrometry is the measurement of the optical intensity from the photons that, through scattering, found its way back to the surface where upon the light was

first induced. It is believed that the measurements obtained through optical spectrometry will be able to give an indication of the concentration of plasma osmolality or water content in the skin through non-invasive and in vivo means. This section gives an introduction to the theory of optical spectrometry and its applicability to work as an hydration marker. The behaviour of photons in several mediums are investigated and assumptions is made based on their behaviour. The mediums under investigation include blood, the different layers in skin and lipids.

2.5.1 Theory

Optical spectrometry is based on the potential of a medium to absorb, scatter and reflect light [28]. This is best described by how we perceive the world. If one were to look at a blade of grass one would perceive the colour green. This is because, due to its optical properties, grass absorbs all wavelengths except the wavelength related to the colour green. What the observer does not notice is that the reflected light has an entire spectrum full of different wavelengths which are unique to the blade of grass. One would be able to shine a set of wavelengths onto a medium and measure the reflection and depending on the intensity of the different wavelengths in the reflection one would be able to identify the medium or make accurate assumptions about the medium. With tissue the concept is the same with the exception that the medium under investigation is a combination of blood, lipids, dead skin cells etc. Here follows the description of the different parameters related to photon behaviour.

The optical properties of a medium are defined by several parameters, namely:

Absoption Coefficient (μ_a) This parameter describes the medium's potential to absorb energy from a photon. This is most commonly seen in the form of Beer's law that gives transmitted intensity (I) as a function of initial intensity (I_0), the length the photons have travelled in the medium (l) and absorption coefficient (μ_a)[29, 30].

$$I = I_0 e^{-\mu_a l} \tag{2.1}$$

Where μ_a can be defined as a function of the volume density of absorbing elements (ρ_a) and the absorption cross-section (σ_a), namely:

$$\mu_a = \rho_a \sigma_a \tag{2.2}$$

It is necessary to note that the absorption coefficient is dependent on the concentration of absorbing elements. If the medium under investigation would undergo a concentration change the absorption coefficient will too change. That is, the more absorbing chromophores present in

the medium the more energy will be absorbed from the photons and with fewer chromophores in the medium the less the energy will be absorbed.

Scattering Coefficient (μ_s) This parameter describes the amount of scattering the photon will undergo in a medium. Scattering occurs due to the fluctuations of refractive index n. This could be due to the morphology, density and size of the particles found in tissue [29, 31]. Scattering plays an important role in the behaviour of photon interaction, determining where the photon absorption will occur [29].

Anisotropy Factor (g) The anisotropy factor is the ability of a photon to keep moving forward after it has undergone scattering [29]. As described by Jacques et al. if the trajectory of a scattered photon is deflected with an angle, the cosine of that angle will give the forward component of said trajectory [29]. The average cosine of a medium's average deflection angle is known as the anisotropy [25]. The anisotropy can range from -1 to 1 which represents back scattering and forward scattering respectively [31].

Refraction Index (n) As is well-known when light encounters a medium with a different refractive index the light will undergo reflection and refraction. This property is a determining factor when working with different mediums or taking into account the, mostly unavoidable, air to medium interaction.

The above-mentioned parameters describe the behaviour of photons in a medium and each plays an important role in identifying the properties of the medium under investigation. It has been shown by Friebel et al. that the change of blood characteristics namely a change in haematocrit, blood osmolality and haemoglobin, will alter these parameters [24]. It is thus assumed that dehydration can be measured by extracting the optical parameters associated with plasma osmolality as it has previously been mentioned is the best known marker for dehydration. It can also be assumed that when in a state of hypovolemia vasoconstriction mechanisms will restrict blood flow to the skin and the skin will exhibit a water deficiency in comparison with the rest of the body [13]. The optical characteristics of the skin can thus play a role in the identification of a person's hydration status. It is important to investigate the optical properties of the skin as to make appropriate assumptions with regards to the wavelengths that should be used for measurements and which layers of the skin will have the larger effect on measurements.

2.5.2 Skin

The skin is a strictly inhomogeneous medium, being a distribution of several chromophores [25, 32]. It is thus necessary to investigate the different layers in

the skin to make reasonable assumptions with regards to how hydration can be measured using optical spectrometry. The skin consists of three different layers; the epidermis, dermis and adipose subcutaneous fat [25].

Epidemis The epidermis, with a thickness of 50-100 μm, consists of two sub-layers namely a non-living layer, called the stratum corneum, and the living layer containing melanocytes responsible for the creation of melanin [25, 30]. Melanin is responsible for the protection of the skin against UV light and for the colour of different racial groups' skin [30]. Due to the thin layer of the living epidermis it can be assumed that melanin plays a small role in the overall absorption in the skin at long wavelengths [30]. It should also be noted that Gajinov et al. mentions that the effect of three different racial groups had a similar absorption magnitude past 900 nm [33]. This is fortunate seeing as measurements past this wavelength can be considered to not be racially biased.

The stratum corneum acts as a protective barrier to the underlying tissue. The stratum corneum is on average 15–20 µm thick and as mentioned in Section 2.4 is hygroscopic, meaning it has the ability to absorb and retain water. There is no blood flow in the epidermis layer and it can be assumed that the stratum corneum has a very low water concentration. The water concentration that is present in the stratum corneum could be due to transepidermal water loss [20] or be due to environmental humidity. Hachiro et al. [20] mentions that TEWL in the skin is but $5\,g/m^2\,h$ showing the low water concentration of the skin due to TEWL. With the latter known and given the thickness of the stratum corneum one can assume that it will have negligible effect on accurately measuring water concentration in deeper tissue.

Dermis This layer, also known as the vascular layer, is approximately 1–4 mm thick and contains blood vessels and is the first layer of the skin to contain blood [25, 30]. It is also said that the dermis consists of 65–75% of water. In the visible spectrum the main absorbers of the dermis are haemoglobin, carotene and bilirubin. More interestingly the main absorbers in the IR spectrum is water [25]. Bashkotav et al. [25] argues that the dermis' water content and dermis' haemoglobin content together with the lipid absorption in the epidermis layer, define the absorption properties of the whole skin.

Two layers of the dermis is responsible for the scattering properties of the layer, namely the papillary dermis and reticular dermis [34]. The papillary dermis is described as exhibiting backscattering properties due to the small size of the collagen fibres therein [34]. The reticular dermis exhibits forward scattering due to the large collagen fibres found therein [34]. It is mentioned by Bashkatov et al. [34] that light that passes this layer will propagate into further tissue and will contribute to some extent

to the reflected spectrum of the skin. The average scattering properties of the skin can be attributed to the reticular dermis due to its thick layer and the comparable scattering properties of the epidermis and reticular dermis. [25, 34]

Subcutaneous Adipose Tissue The subcutaneous layer is 1–6 mm thick consisting of the aggregation of fat cells (adipocytes) containing droplets of fat (lipids) [25, 34]. These cells are surrounded with connective tissue, blood capillaries and nerves that provides metabolic activity for the subcutaneous layer up to the dermis layer [25]. This layer's main absorbers are water, lipids and haemoglobin [25]. The main scatterers of this layer is the spherical droplets of lipids distributed within the adipocytes.

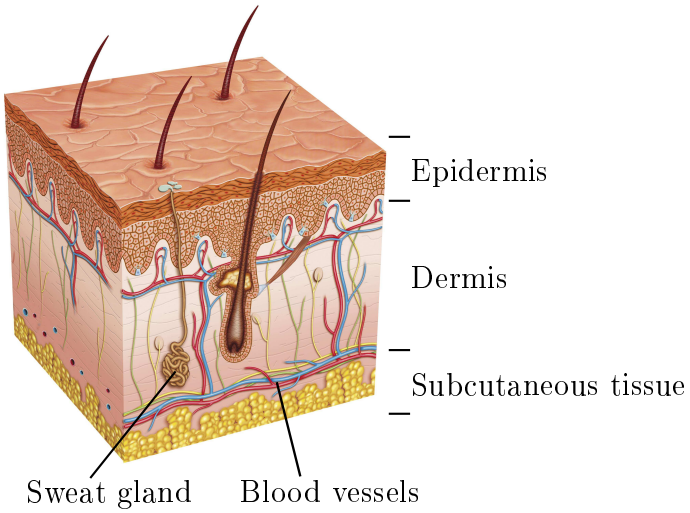

Figure 2.7: Layers of skin: epidermis, dermis and subcutaneous tissue [2].

It was decided that absorption will be used as the basis of measurement for the IR device as the literature regarding the absorption properties of skin is numerous and showed greater diversity in spectral characteristics than that of the scattering and the refractive index properties of the skin. As mentioned above the main absorbers in the skin in the IR spectrum are water, lipids and haemoglobin. To make it possible to measure water concentration it is necessary to measure in this spectrum. Haemoglobin and lipids are still present and it is necessary to investigate the spectrum of these chromophores as well as to choose a wavelength where the absorbing coefficient of water is dominant so that lipids and haemoglobin can be assumed to be negligible. Figure 2.8 gives the spectrum of water lipids and haemoglobin.

As can be seen from Figure 2.8 water becomes the dominant absorber in the wavelength range of 1250 nm and onwards. Further it can be seen that

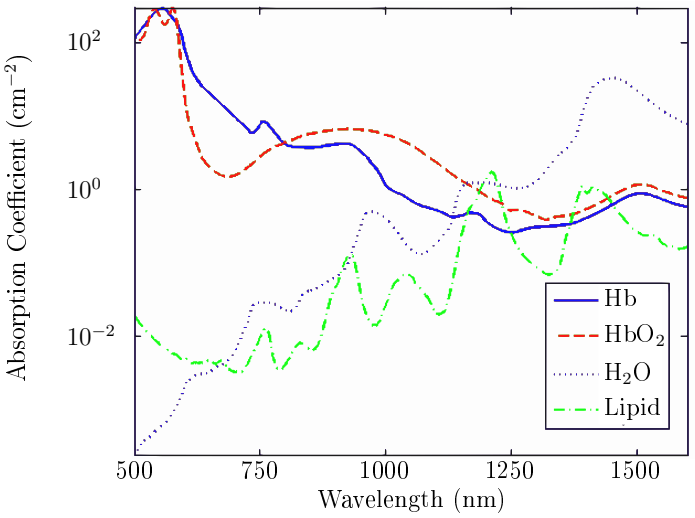

Figure 2.8: Optical absorption coefficient of deoxyhaemoglobin, oxyhaemoglobin, water and lipids [3]

haemoglobin and lipids decreases in absorption. Given the decreased absorption of haemoglobin and lipids and that measured light intensity is an exponential function of absorption it can be assumed that the measured intensity of the skin can be approximated as a function of water concentration alone.

2.6 Hypothesis

With the theory of BIA, SC impedance and IR spectrometry reviewed, a number of hypotheses can be made.

1. It is postulated that BIA analysis can be used to investigate the change in extracellular fluid due to dehydration and that this marker for dehydration can be used to develop a device that can be used as in infield tool for measuring dehydration.

2. Stratum corneum impedance analysis can be used to evaluate the transepidermal water loss in the skin by measuring the water content in the stratum corneum by measuring the impedance of the stratum corneum.

3. It is believed that infrared diffuse spectrometry can be used to evaluate the concentration of plasma in the skin's blood which is sensitive to hypertonic hypovolemia and/or it can be used to measure the overall water concentration of the skin which is sensitive to isotonic hypovolemia due to the vasoconstriction mechanisms in the body.

4. It is postulated that Bioimpedance analysis together with the stratum corneum impedance analysis and infrared spectrometry devices will yield measurements that will coincide with the hydration state of an infant and this will remain possible even in the face of its in vivo capabilities (see objectives). As a secondary hypothesis it is believed that the devices can be used for adults as well.

2.7 Chapter Summary

This chapter presented a literature review of the different methods that will be incorporated in the design of three dehydration assessment devices. An introduction to existing hydration markers was given and the shortcomings of the markers were discussed. These shortcomings were due to the marker's inability to work as an infield measuring device for dehydration. In addition to this the cost, portability and required technical expertise of each marker was given and it was seen to be in contrast with the objectives of this project. The theory behind BIA and SC impedance analysis was given as well as a brief insight to the workings of optical behaviour. Lastly with the collective knowledge of the different methods hypotheses were made postulating the abilities of the different methods.

Chapter 3

Device Design and Implementation

3.1 Device Descriptions

As mentioned in the previous chapter bioelectrical impedance analysis, stratum corneum impedance analysis and infrared spectrometry will be used to identify dehydration in a person. Here follows the description of the fabricated devices and how they will be implemented. The data sheets for the different components mentioned in this section can be found in the appendix.

3.1.1 BIA

Many BIA analysis devices exist and have been used as a standard device for several studies. An example of such a device is the Xitron Hydra used by Röthlingshöfer in "Monitoring Change of Body Fluid during Physical Exercise using Bioimpedance Spectroscopy and Finite Element Simulations" [15]. It was aimed to produce an inexpensive way to measure the bioimpedance of the body and it was thus opted to design a low current BIA device safe to use on infants. This was done through the use of a direct digital synthesizer (DDS) module, microcontroller and some analogue circuitry (discussed in more detail in Section 3.2.1). The microcontroller enables the DDS module to generate a sinusoidal signal which is lead to the skin through a coaxial cable attached to two disposable pre-gelled ECG electrodes. These electrodes are placed upon the ankles of the subject and the impedance is measured forthwith using the analogue to digital converters (ADC) of the microcontroller.

3.1.2 SC Analysis

There already exists a number of stratum corneum probes namely the Skicon 200 and Corneometer CM 825. As mentioned in the objectives of this project it is sought to use inexpensive technologies and it was thus decided to use the method incorporated by Hamed et al. [8]. Hamed et al. conducted a study using a double circular electrode comprising of copper, and showed that

Figure 3.1: Stratum corneum probe encapsulated in silicon with coaxial cable attached

hydration in the stratum corneum was indeed measurable and that it showed a good correlation in comparison to the Corneometer. It was thus decided that the probe used by Hamed et al. will be used for this project.

As described by Hamed et al. the probe consists of circular copper rings printed onto a circuit board. Figure 3.1 shows the probe with the inner electrode having a diameter of 6 mm and outer electrode having an inner diameter of 10 mm and outer diameter of 12 mm. These electrodes were relayed via a coaxial cable to the measuring hub described in Section 3.2.1.

3.1.3 Infrared Spectrometry

As mentioned in Section 2.5 infrared is a very advantageous spectrum to work with in the case of water concentration measurement. This is due to the high absorption capabilities of water in this spectrum. There do however exist other major absorbers in this spectrum which were taken into account and the wavelengths of interest were chosen in such a way that the absorption will be dominated by water. These wavelengths were chosen at 1300 nm and 1480 nm. These wavelengths were chosen purposefully so that the 1300 nm had an absorption coefficient fairly smaller than that found at 1480 nm. This was done because it was believed that with the smaller absorption coefficient the light will be able to travel further and hopefully propagate further into the skin before diminishing to an unmeasurable magnitude. It is also believed that at this wavelength a greater area of tissue will be observed compared to the 1480 nm wavelength. The 1480 nm wavelength was chosen as it was believed that it would be more sensitive to water concentrations given its high absorption coefficient.

These two wavelengths are produced by using specially ordered infrared LEDs provided by Roithner Technik [35]. These are used in conjunction with a photodiode provided by the same manufacturer that measure the spectrum

Figure 3.2: Infrared probe concealed in silicon

between 1000 nm and 1600 nm. The LEDs and photodiode are mounted so that the sensing area of the photodiode and the light inducing area of the LEDs are in the same plane. This is to ensure that when pressed onto the skin all forms of light will be cutoff from the photodiode and the only wavelengths it will measure will be that produced by the LEDs. Other forms of circuitry is needed to operate the LEDs and the photodiode but this is shown in Section 3.2.2.

An overview of the devices has been given with a summary with regards to design choices made. The following section describes the circuit design of the above mentioned devices in detail.

3.2 Circuit Design

For this project it was necessary to design certain circuitry to implement the sensors as described in Section 3.1. The circuitry involves the buffering and amplification of small voltage signals produced by the BIA and SC devices. With regards to the IR device it is necessary to amplify the small currents produced by the photo-diode and to power the LEDs via the microcontroller. In addition to the last mentioned a voltage splitter and regulator was build and implemented to power the amplifiers, buffers and LEDs.

3.2.1 BIA and SC Impedance

It was decided that with the design of the BIA and SC sensor that the circuit will make use of a voltage division between the body and a known reference resistor, namely 56 kΩ. This reference resistor was chosen for the sake of electrical safety as defined by the IEC60601-1 standard. This was to ensure that even under no load conditions the subject will be subjected to a current far under the danger threshold for electrical shock. It was chosen to design conservatively with regards to current as the author exercised caution with

what the infants will be subjected to during the study. This conservatism was spurred on due to an infant's inability to communicate discomfort.

In order to calculate the impedance to signals are measured, namely the reference voltage and the voltage divided signal across the body. This is depicted in Figure 3.3 as x_1 and x_2 respectively. Each measured signal will pass through a buffer to ensure that the integrity of the ADC circuitry of the microcontroller is not compromised by the unknown impedance which could lead to perturbed results and also not to load the circuitry connected to the body. This is made possible due to the buffer's low output impedance and high input impedance. As a precaution, due to the unknown impedance of the different types of tissues, signal x_2 will undergo two amplifications each with magnitude of roughly 20 dB. This was done as to be able to measure possible small impedances. After each amplification stage the signals can be measured with the ADC. Figure 3.3 depicts the voltage division, the buffers and the two amplifier configurations of the BIA and SC circuit.

The LM324 was chosen for the circuit as it is a single IC consisting of four independent operational amplifiers resulting in a simplified PCB design with fewer supply voltage tracks and signal carrying tracks. The LM324 also has a sufficient bandwidth of 200 kHz at a gain of 20 dB which is suitable for the amplification stage of the amplifier. The LM324 also doubles as the buffers for the circuit.

As mentioned it is necessary to calculate the impedance as to derive a Cole–Cole plot to analyse the water content of the body. It is thus necessary to calculate the transfer function of the presented circuit to be able to calculate the unknown impedance body shown in Figure 3.3 as Z_B. The transfer function of the circuit is shown in equation 3.1.

$$\frac{x_2}{x_1}(s) = \frac{Z_B}{sZ_B R_R C_{cable} + R_R + Z_B} \tag{3.1}$$

From equation 3.1 it is possible to derive the impedance of Z_B.

$$Z_B(s) = \frac{x_2 R_R}{x_1 - s x_2 R_R C_{cable} - x_2} \tag{3.2}$$

More detail about the calculation of the impedance through signal analysis is discussed in Chapter 4.

3.2.2 Infrared Spectrometry Circuit

The IR circuit is depicted in Figure 3.4. A photo-diode was used for measuring the intensity of IR light. This was decided seeing as how the photo-diode boast a near linear behaviour with regards to producing current from light. This photo-device unfortunately has a disadvantage, which is the small current it produces even when subjected to a high intensity light source. It was

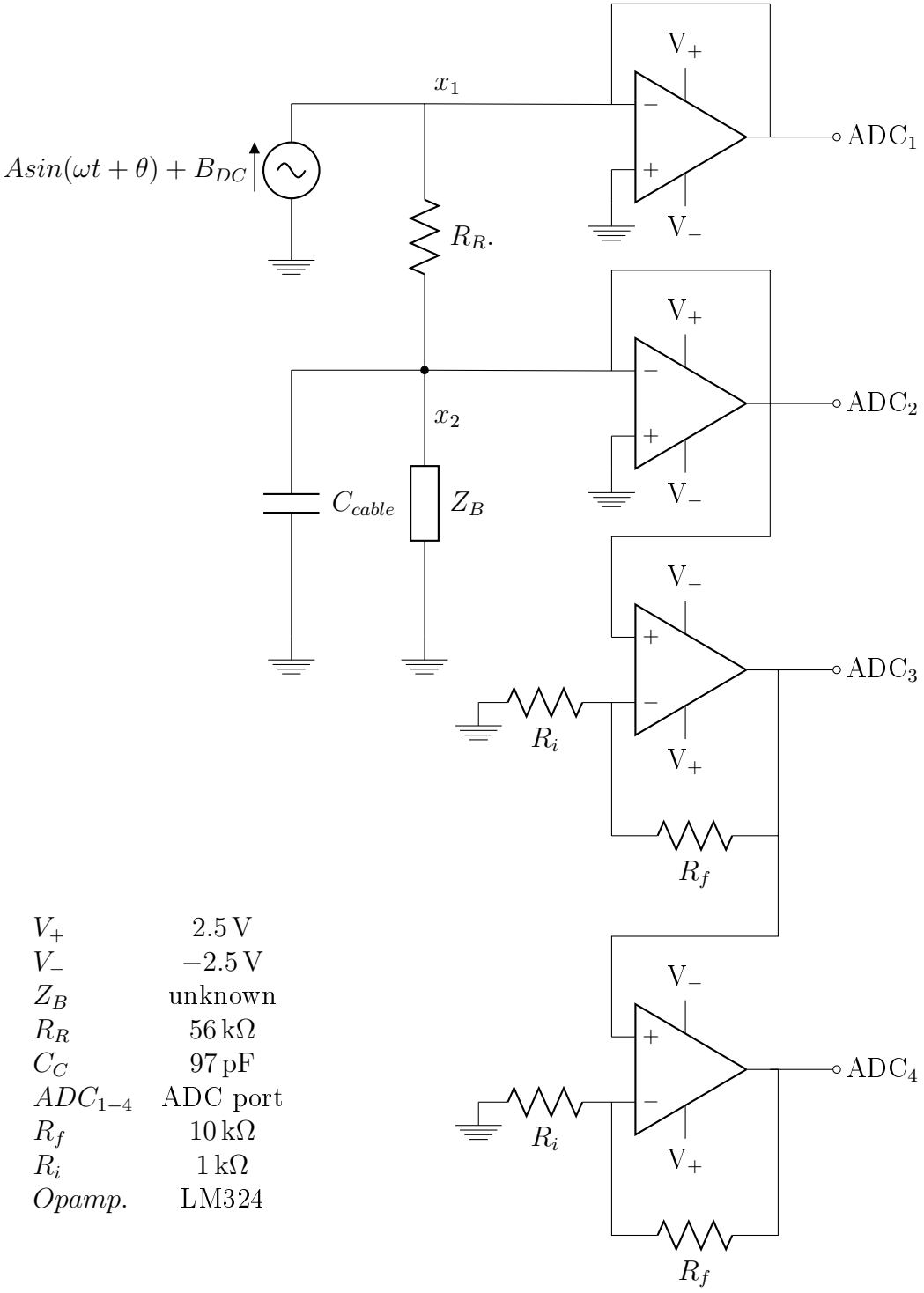

V_+	2.5 V
V_-	−2.5 V
Z_B	unknown
R_R	56 kΩ
C_C	97 pF
ADC_{1-4}	ADC port
R_f	10 kΩ
R_i	1 kΩ
Opamp.	LM324

Figure 3.3: BIA and SC circuit configuration

thus necessary to amplify this current and find a resulting voltage that is measurable with the microcontroller. It was decided to make use of a photovoltaic amplifier configuration as seen in Figure 3.4. There are different photodiode

configurations available but this one was chosen due to its ability to suppress dark current. Dark current is the leakage current produced by a photodiode under no illumination conditions. Dark current is a function of temperature and its biased voltage. Dark current can thus influence readings making it a perturbing factor which was taken into account when choosing the circuit configuration. In the photovoltaic configuration the dark current is minimised to the point where it can be seen as negligible and with this assumption it can thus be assumed that the generated current is the product of light intensity only. The equation governing the behaviour of the amplifier is given in equation 3.3.

$$\frac{V_{out}}{i_{sc}} = \frac{R_G}{sR_GC + 1} \tag{3.3}$$

where i_{sc} is a linear function of received light.

The photodiode used for the circuit is the IPD14-12-5T which can measure in the spectrum range of 1000 nm to 1600 nm. The photodiode can thus measure both the wavelengths of the LEDs resulting in fewer measuring components. Only one photodiode was incorporated in the design as the shared amplifier configuration will result in both wavelengths being amplified with the same gain, thus lending some robustness to the statistical relevance of the measurements. The photodiode also boasts a high responsitivity to light giving

$$i_{sc} = 0,9P \tag{3.4}$$

where P is the intensity of light measured in watt.

The photovoltaic configuration amplifies the current produced by the photodiode with a magnitude equal to the resistor (R_G). The photo-diode was tested with various resistor values and it has been found that a 10 MΩ resistor resulted in a favourable gain, enough as not to lose information due to the voltage cutoff brought on by the amplifier. The added capacitance adds an additional pole to the system that acts as a low pass filter making the circuit stable and more robust against oscillations. This value was chosen as 100 nF.

To investigate the absorption of infrared light due to water concentration two diodes were used to shine two wavelengths of IR light into the skin. The photodiode is used to measure the intensity of the diffuse light giving the sought indication. Due to the microcontroller only being able to output 18 mA of current a transistor was used as a switching mechanism for the diodes as to provide a current higher than that of the microcontroller from the voltage supply. The transistor and LED configurations are shown in Figure 3.4. The circuit was designed to achieve a diode current of 40 mA. The LEDs used in the design are a 1300 nm and a 1480 nm wavelength LEDs provided by Roithner Technik [35]. The LEDs were given preference due to them being inexpensive which is one of the objectives of this project; making the devices affordable for underserved communities.

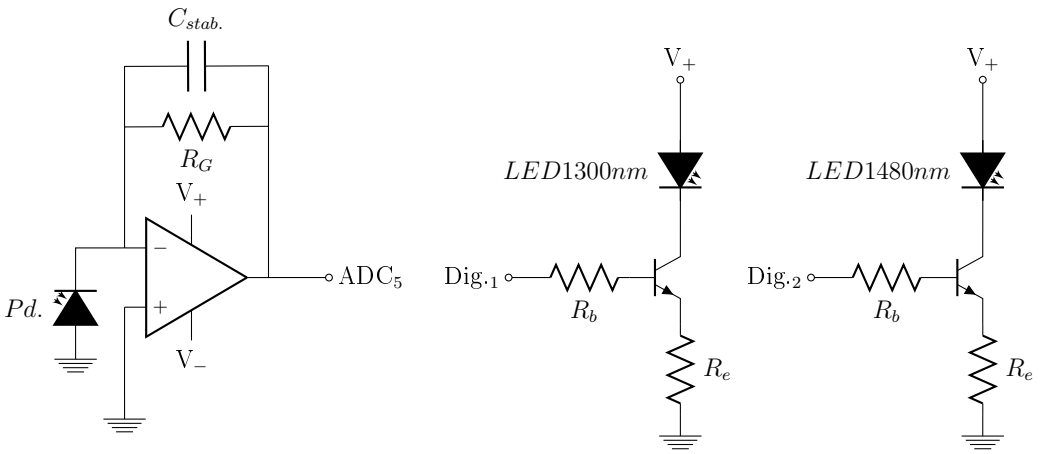

V_+	2.5 V	ADC_5	ADC port
V_-	−2.5 V	$Dig._{1,2}$	Digital port
R_G	10 MΩ	$LED1300$ nm	LED1300-series
R_b	3 kΩ	$LED1480$ nm	ELD-1480-525
$C_{stab.}$	100 nF	$Pd.$	IPD14-12-5T
R_e	36 Ω	$Opamp.$	TS912ID

Figure 3.4: IR and LED circuit configuration

3.3 Voltage Supply

It is necessary to implement a voltage supply splitter with the use of the amplifiers. This was to find a common ground between the signals and the microcontroller. In doing so the cutoff voltage was increased as the signals from the amplifiers are no longer centred around half the amplifiers' supply voltage but around the ground of the microcontroller, enabling the full use of the ADC of the microcontroller. The supply splitter needed to be robust, keeping voltage well regulated whilst being able to deliver and handle high currents drawn by the amplifiers, LEDs etc. A supply configuration was found and is shown in Figure 3.5. This configuration is described as being able to handle currents up to 1.5 A whilst keeping the ground steady at half of the supply.[1]

3.4 Digital Interface

This section describes the interconnectivity of the previous section's analogue circuits with that of the digital interface. This interface includes a microcontroller, WIFI module and direct digital signal synthesizer. This section explains the role of all the digital components, how they work and their limitations.

[1]Designs can be found at http://www.head-fi.org/t/654485/virtual-ground-regulated-and-rail-splitter-circuits

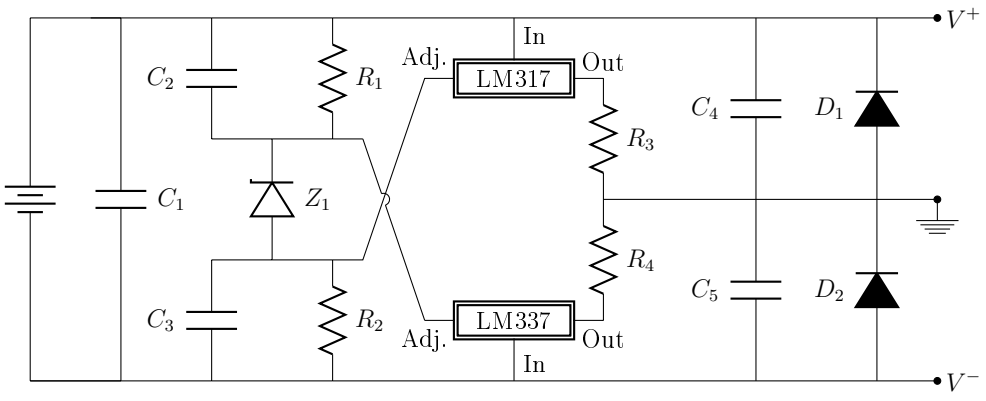

C_1	470 µF	C_4, C_5	1000 µF	Z_1	LM336
C_2, C_3	22 µF	D_1, D_2	1N4004		
R_1, R_2	1.8 kΩ	R_3, R_4	1 Ω		

Figure 3.5: Voltage splitter and regulator

3.4.1 Microcontroller

It was aimed to create a portable device which could be implemented as a standalone hydration sensor. It was thus decided that use will be made of a microcontroller to implement the signal sampling, signal analysis, various calculations, control of various components and communication via WIFI to a PC. All the devices are connected to this microcontroller which was chosen to be an Arduino Uno32. This microcontroller was chosen due to its fast clock speed (80 MHz) and its fast sampling speed (1MSPS). Though many devices do exist with higher sampling rates and larger memory the microcontroller was given preference seeing as the IC alone only costs around 50ZAR. It was sought to make the devices affordable for underserved communities so the decision was made to continue with the UNO32 in the project.

The microncontroller has been fitted with a WIFI module to establish wireless communication with a computer. With each iteration of measurements the microcontroller would send data via the WIFI to the computer which in turn would categorize the data and save it to a comma separated file. This was necessary for data handling and giving the microcontroller unhindered portability whilst still being able to investigate the captured data sent to the computer. This enabled the user to investigate the results of the measurements making it possible to pick up on any faults.

The Arduino UNO32, though powerful for a microcontroller in general, exhibited a few limitations. The most detrimental limitation is its method of sampling. The microcontroller does indeed have a 1 MSPS speed but this is its maximum sampling speed applicable to a single ADC channel. The maximum sampling speed is a function of the number of channels in use. If two channels were to be used a maximum sampling speed of 500 kSPS could

be expected. The sampling is also done sequentially and hence required phase calibration (see Section 4.2). Apart from the sampling limitations the Arduino UNO32 houses a PIC32 microcontroller chip which has been preprogrammed by Arduino to reduce the difficulty factor of the PIC32 for microcontroller enthusiasts. This was found to be counter intuitive as the microcontroller had to be redundantly reprogrammed as to reprogram the Arduino's programming. This was the case whilst configuring the sampling speed of the microcontroller seeing that Arduino's programming only allows a maximum sampling speed of 10 kHz and it was thus necessary to reprogram the microcontroller via the PIC32's original code.

3.4.2 Direct Digital Signal Synthesizer (DDS)

When implementing the BIA analysis device or the SC impedance analysis device it is necessary to induce a current in the subject which can be measured and analysed via Fourier analysis. For the purposes of this project a signal synthesizer was used for its ability to digitally produce sinusoidal signals. This is very advantageous when implementing Fourier analysis as a sinusoidal signal will result in only two impulses in the observable spectrum which eases signal processing (see Chapter 4). The AD9850 was used for this purpose as it produces a near ideal sinusoidal up to frequencies of up to 62.5 MHz with negligible error. For the purposes of this project the frequency did not exceed 200 kHz due to the sampling limitations of the microcontroller. The DDS is powered and written to via the microcontroller. The microcontroller sends a 40-bit data string which holds information regarding the frequency, phase and other configuration bits pertaining to the operation of the DDS. When received the DDS produces the sinusoidal wave immediately.

3.4.3 WIFI Module

As mentioned the microcontroller was fitted with a WIFI module as to communicate with a PC for data quality reassurance. The Microchip MRF23WB0MA shield from Digilent is used. This module is capable of transmitting over distances of 400 meters at a maximum rate of 11 Mbps or 54 Mbps for 802.11b and 802.11g transmission rates respectfully. This shield was also chosen due to its compatibility for the Arduino Uno32.

3.5 Analogue and Digital Interconnectivity

As mentioned all the devices and digital components are controlled via the microcontroller which allows for the interconnectivity amongst these components. Figure 3.6 shows a diagram depicting the interconnectivity of all the components both analogue and digital.

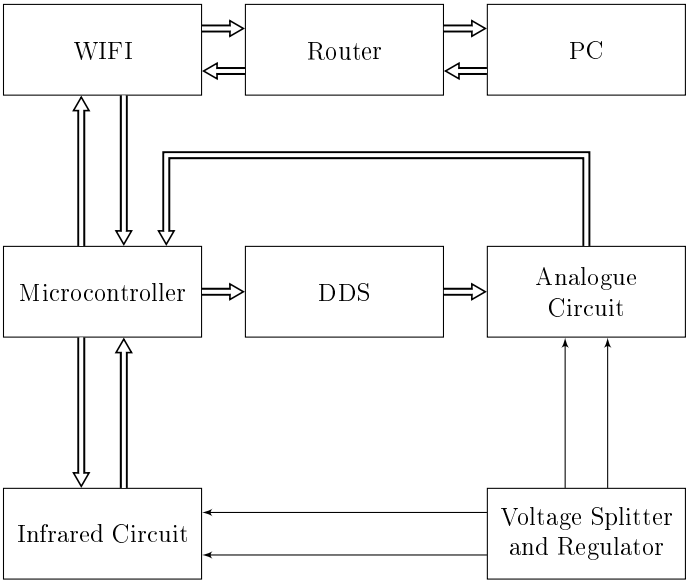

Figure 3.6: Overview diagram of digital setup

3.6 User Interface

When the devices have measured and processed the data, the results are sent via WIFI to a PC where it is shown in a graphical user interface (see Figure 3.7). This GUI was developed in Qt Creater 5.2 which is a cross platform programming development environment with its own graphical editor for making applications. The GUI is programmed to implement pushbuttons to send commands via WIFI to the microncontroller to execute functions. The GUI also has the capabilities to catalogue and store the information sent to it in comma separated value files. The main function of the GUI is to display the measured results for quality reassurance and to organise and store the measured data. The following describes the functions of the different sections as numbered in Figure 3.7.

1. Each subject is given an I.D. number which corresponds to the subject and the number of the test. These I.D.'s were pre-written to a text file and read into the GUI upon start-up of the program. Upon testing the subject the I.D. of the subject is chosen and will appear under "subject" shown in number two in the figure. Upon successfully saving the data the test number of the I.D. is iterated by one and saved to the text file for the next test to be performed on the subject.

2. Upon choosing the subject I.D. it will appear in the textbox situated under "subject" shown in the figure. This I.D. will be saved at the end of the data acquisition process upon pressing "Save Data". A text box

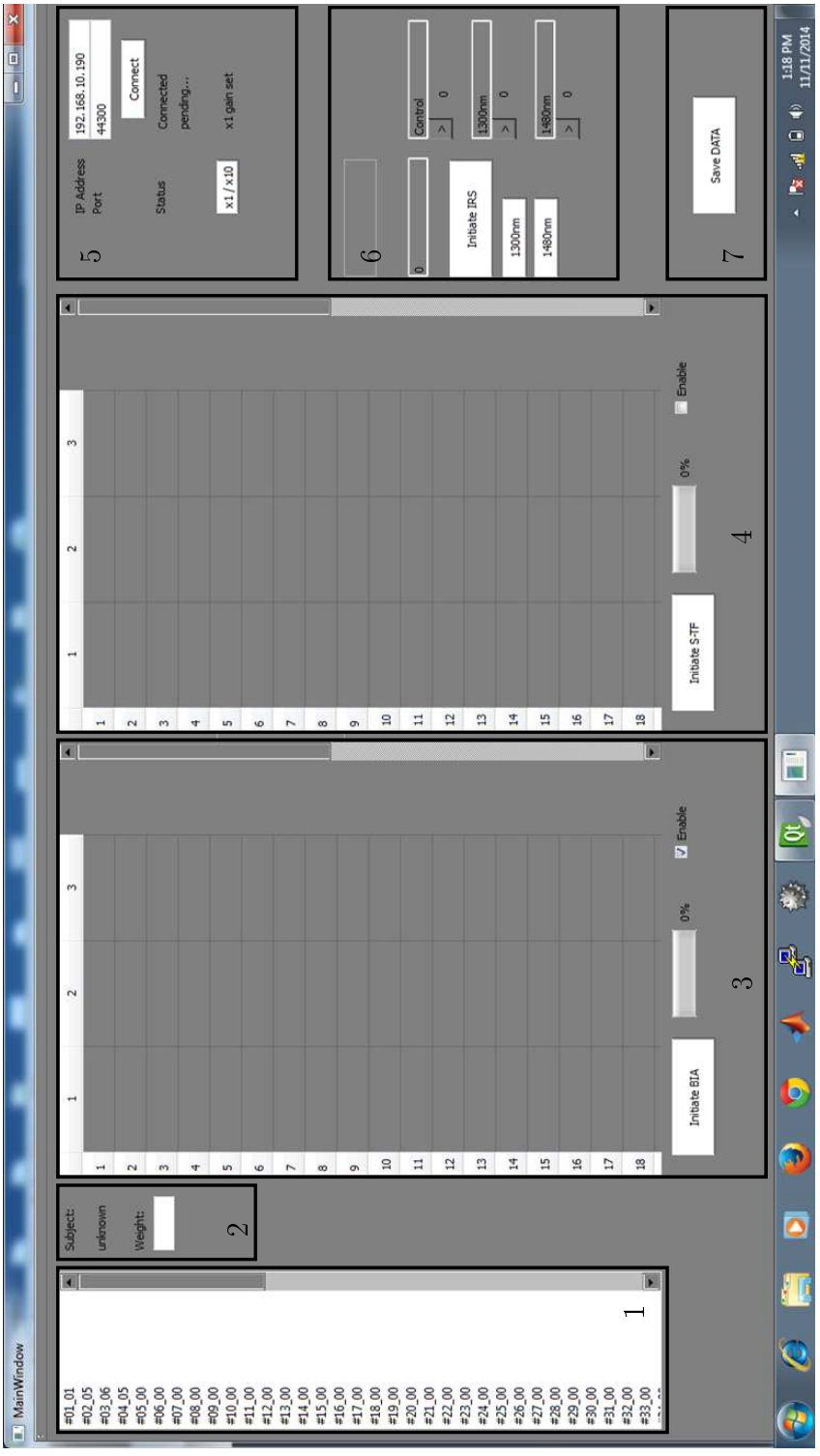

Figure 3.7: User interfaced programmed with Qt Creator

is provided to include the measured weight of the subject. This is also saved together with the subject I.D.

3. Once the "Initiate BIA" button is pressed the GUI sends a character via WIFI to the microcontroller. Once recognised the microcontroller will start measuring the ankle to ankle impedance of the subject. Once measured the array of data is send to the GUI which is then displayed in the table. The first column of the table will give resistance, the second column the reactance and the last column will give the frequency at which the measurements were taken. As the data is send the progress bar will fill to 100% after which other measurements can be taken. An enabled check box is included to enable or disable the BIA procedure. This is to inform the save procedure to omit the data from the saving procedure.

4. Similar to point 3 above, a character is sent to the microcontroller and upon recognising the character the microcontroller initiates its impedance measuring protocol. The progress bar and enable check box works similarly as described above.

5. This section displays the information needed to connect to the microcontroller via WIFI. The IP address of the microcontroller and the applicable connection port is defined and used to connect to the microcontroller when the "Connect" button is pressed. The status labels show the status of the connection. The status shows if the GUI has successfully connected to the microcontroller and if the GUI is reading or writing information from or to the microcontroller. The button labelled "x1/x10" is used to switch between unity amplification and 20 dB amplification.

6. This section describes the GUI for the infrared spectrometry protocol. All the buttons in this section are toggle buttons. Once toggled a character is sent to the microcontroller that, when recognising the character, will start the desired action. If the button is toggled again a character will be sent that will stop the process. When "Initialize IRS" is toggled it will begin the infrared spectrometry protocol on the microcontroller. This protocol enables the microcontroller to send measurements continuously and will only stop once the button has again been pressed. The measurement data sent during this process appears in the textbox situated above the "Initiate IRS" button. With each new data packet the previous measurement will be replaced by the new one. While the measurements are being sent the buttons 1300 nm and 1480 nm can be toggled to switch on the corresponding IR LED's. If the buttons are to be pressed again the LEDs will switch off. Once the measurement has stabilized the ">" button is pressed to log in the measurement into any of the three text boxes labelled control, 1300 nm and 1480 nm.

7. Once all data has been logged the "Save Data" button is pressed to save all data to their corresponding directories. Directories are created in such a manner that each subject has its own folder with BIA, SC and IR subfolders housing the different iterations of measurements. All measurements are saved in comma separated files in the last mentioned folders.

3.7 Chapter Summary

In this section the different digital components of the digital interface were discussed as well as the limitations of said components. In the previous section the analogue circuits of the devices were viewed and their connectivity to the digital interface was also discussed. When implementing the devices to take measurements all these components, analogue and digital, work in unison to produce and send the measured information to a computer which implements a graphical user interface to view the information for quality reassurance.

Chapter 4

Signal Processing

In order to calculate tissue impedance it is necessary to obtain the attenuation and phase of the signals as described in Chapter 3. It has been decided to use the Fourier transform to obtain the necessary information to calculate the tissue impedance. This section describes the use of the discrete Fourier transform and its implementation in determining the tissue impedance of a person.

4.1 Discrete Fourier Analysis

The following equation defines the discrete Fourier transform.

$$X[k] = \sum_{n=0}^{N-1} x[n] \cdot e^{-i\pi kn/N} \tag{4.1}$$

where X_k is the Fourier transform of the signal x_n with N samples, and k denotes the frequency component of the transformed signal and n the sample of the signal in question. As can be seen from equation 4.1 the discrete Fourier transform proportionally takes N^2 operations to calculate the entire bandwidth of the signal in question. This presents a problem when using a microcontroller with a slow clock speed and fairly limited memory. It was thus necessary to program the signal processing algorithm in such a way as not to be hindered by the microcotroller's limitations. The limitations being the saturation of the microcontroller's small memory and the processing speed of the microcontroller not being too long and becoming a hindrance in the validation and testing stages of the device. Fortunately the frequency of the DDS signal is known. This could significantly reduce the number of operations of the Fourier transform to only N operations seeing as the frequency component (k) of X_k is known by using equation 4.2 which describes the relationship

between the signal frequency, sampling frequency, number of samples and the frequency component.

$$k = N \cdot \frac{f}{f_s} \tag{4.2}$$

where f is the frequency of the signal being sampled and f_s is the sampling frequency of the microcontroller.

Unfortunately it was found that the sampling speed of the microcontroller was unreliable and was subject to change. It was believed that this was caused by conflicting programming from the Arduino environment. This caused the frequency component of the transformed signal X_k to shift. The reason can easily be seen from equation 4.2. By assuming that the number of samples of the signal and the frequency of the signal will stay constant it can easily be seen how a change in sampling speed will change the frequency component. The signal processing algorithm was thus altered to accommodate the possible frequency shift of the transformed signal X_k. The algorithm calculates the expected frequency component of the signal x_n and using this expected frequency component will calculate the Fourier transform of the other two frequency components to either side of it. From the five Fourier transforms the component with the highest magnitude will be identified as the dominant harmonic related to the signal x_n.
Equation 4.3 to 4.10 describes the calculation of the impedance given the two measured signals.

Two signals are sampled by the ADC giving the signals $x_1[n]$ and $x_2[n]$.

$$x_1[n] = Asin(2\pi \frac{f}{f_s}(n - C)) \tag{4.3}$$

$$x_2[n] = Bsin(2\pi \frac{f}{f_s}(n - D)) \tag{4.4}$$

Given that the signals are strictly sinusoidal it is expected that the Fourier transform of the signals will be two impulses over the perceivable bandwidth located at the frequency component K, where $K = N\frac{f}{f_s}$. The magnitude of these impulses are given by equation 4.5 and 4.6.

$$\Big|\big|X_1[k]\big|\Big| = \frac{AN}{2}\Big(\delta[k - K] + \delta[N - k + K]\Big) \tag{4.5}$$

$$\Big|\big|X_2[k]\big|\Big| = \frac{BN}{2}\Big(\delta[k - K] + \delta[N - k + K]\Big) \tag{4.6}$$

Using signal $x_1[n]$ as the reference signal its phase is kept at 0 rad. The difference in phase between signal x_1 and x_2 is assigned to signal x_2. The

phase difference of the signal is procured by finding the angle of the transform at $X_1[K]$ and $X_2[K]$.

$$\phi_{x_2} = \angle X_2[K] - \angle X_1[K] \tag{4.7}$$

Using the information obtained from the Fourier transform it is possible to write the signals x_1 and x_2 in polar form:

$$x_1 = A\angle 0 \tag{4.8}$$

$$x_2 = B\angle\phi_{x_2} \tag{4.9}$$

Using the now known signal phasors the impedance can be calculated using the equation derived in Chapter 3:

$$Z_B(j2\pi f) = \frac{x_2 R_R}{x_1 - j2\pi f x_2 R_R C_{cable} - x_2} \tag{4.10}$$

4.2 Signal Phase Calibration

It was initially sought to investigate tissue impedance in the range of 100 Hz to 200 kHz and it was thus necessary to find a microcontroller with a fast enough sampling potential. This lead to the use of the Arduino Uno32 which has a maximum sampling speed of 1 mega sample per second (MSPS). This microcontroller samples sequentially and it was thus necessary to calibrate the phase shift that is present between the two measured signals. As mentioned in the previous section the sampling clock is unreliable and this could influence the phase difference between the two signals. In this case it will be necessary to first calculate the expected dominant frequency component of the signal and follow the Fourier transform method as explained in the previous section. Once the dominant frequency has been found it is used to calculate a better estimate of the sampling speed of the microcontroller. Once the sampling speed is known it is possible to calculate the phase shift between the two signals.

Figure 4.1 demonstrates how equation 4.11 and 4.12 was derived.

Let it be assumed that the device samples two analogue signals of equal magnitude and phase, illustrated in the Figure 4.1 as the black continuous line. The microcontroller samples the signals with a frequency F_s, shown by the red and blue stems, where the blue stems are the samples of signal x_1 and the red stem are those of signal x_2. It would seem that signal x_2 has been shifted to the left resulting in a phase shift relative to signal x_1. This phase shift is the fraction of the sampling period over that of the signal period times 2π. Equation 4.11 and 4.12 gives the phase shift due to sequential sampling.

$$\theta_{disp.} = 2\pi\frac{f}{F_s} \tag{4.11}$$

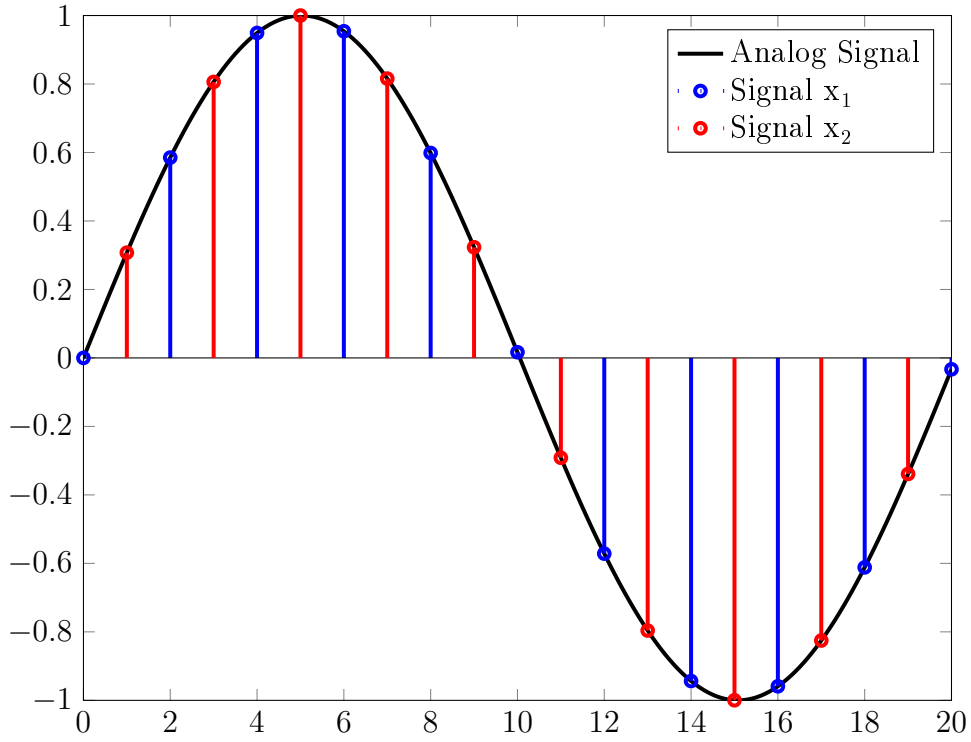

Figure 4.1: Sequential sampling of an arbitrary analogue signal to produce the signals x_1 and x_2

$$\theta_{disp.} = \pi \frac{f}{f_s} \tag{4.12}$$

4.3 Circuit Calibration

4.3.1 Cable Capacitance

With the fabrication of the impedance device it was seen that the behaviour of the device was not ideal and that a pole was present in the transfer function. It was later found that the coaxial cable of the device exhibited a capacitance which caused the pole in the transfer function. It was thus necessary to determine the capacitance as to calculate the impedance over the entire frequency range. To determine the capacitance a resistive load was attached to the cable and the voltages were measured over the frequency range of 100 Hz to 200 kHz. These voltages were used to produce a Bode plot off of which the cutoff frequency could be read. This was repeated for several resistor values resulting in several cutoff frequencies. Using the set of resistors and cutoff frequencies the capacitance is easily calculated through a least squares method. It can be

seen from equation 3.1 that the cuttoff frequency is:

$$\omega_c = \frac{R_R + Z_B}{R_R Z_B C_{cable}} \tag{4.13}$$

It is given in equation 4.14 in matrix form ($AC = b$).

$$\begin{pmatrix} \omega_{c,1} R_R Z_{B,1} \\ \omega_{c,2} R_R Z_{B,2} \\ \vdots \\ \omega_{c,n} R_R Z_{B,n} \end{pmatrix} C = \begin{pmatrix} R_R + Z_{B,1} \\ R_R + Z_{B,2} \\ \vdots \\ R_R + Z_{B,n} \end{pmatrix} \tag{4.14}$$

The capacitance is given by:

$$C = (A^T A)^{-1} A^T b. \tag{4.15}$$

4.3.2 Amplifier Calibration

Due to the uncertainty of the measured impedance two amplifiers were utilized as a precautionary step if the voltage x_2 would become too small and fall beneath the minimum measurable voltage of the microcontroller. The chosen amplifier for this project was the LM324. This amplifier was chosen as it seemed at the time to have a bandwidth larger than 200 kHz. This was not the case as factors like temperature and supply voltage was not taken into account resulting in the amplifier exhibiting a narrower bandwidth. An attempt was made to try and calibrate the measurements in the hope of winning back some bandwidth. The method used is very similar to that of the previous section. A resistor was used as a control and then the voltage was measured over the frequency range of 100 Hz and 200 kHz. The voltages were measured from x_2 to ADC_3 (as seen in Figure 3.3) These voltages were used to produce the Bode plots of each of the amplifiers. From the Bode plot the transfer function of the amplifier was found and with it the means to calibrate the amplifier. From the Bode plot it was deduced that the amplifier exhibited behaviour similar to that of a second order low pass filter. The amplifier model is shown in equation 4.16.

$$\frac{x_1}{ADC_3}(s) = \frac{G}{(\frac{s}{\omega_{c1}} + 1)(\frac{s}{\omega_{c2}+1})} \tag{4.16}$$

The transfer function of the amplifier was approached by placing the two poles at $\omega_{c1} = 2\pi 150$ krad s^{-1} and $\omega_{c2} = 2\pi 260$ krad s^{-1}. The amplifier is independent from the appended circuitry due to its high input impedance and the previous buffers low output impedance. The model is thus viable for any value of Z_B. The second amplifier is configured with the same gain as the previous amplifier and has the same characteristics of said amplifier. The model is thus applicable to both amplifiers for calibration purposes.

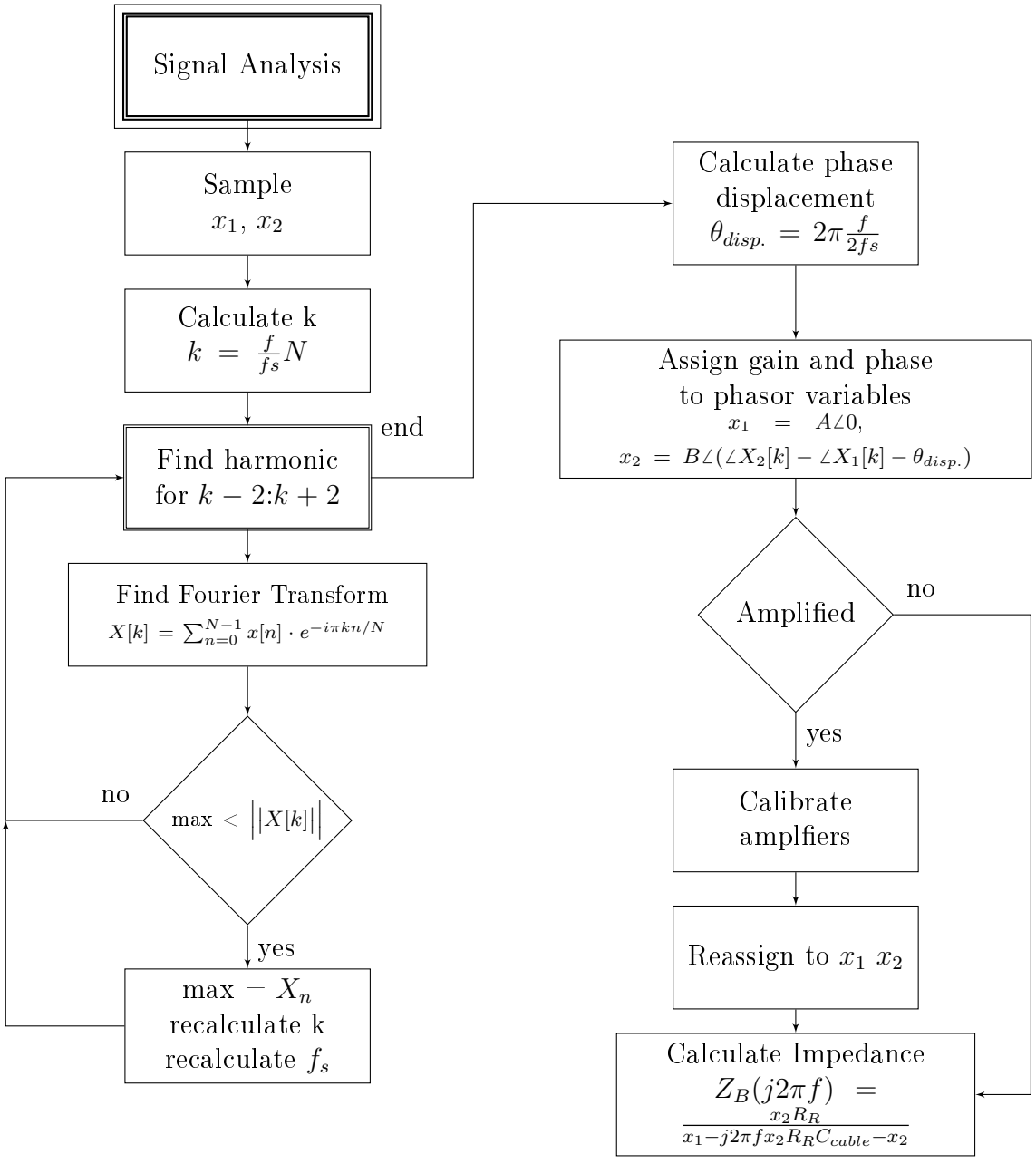

Figure 4.2: Algorithm implemented by the microcontroller to calculate the body impedance

4.3.3 Impedance Calculating Algorithm

The process with regards to the calculating of the impedance is depicted in Figure 4.2. Once the function is called the microcontroller samples the signals x_1 and x_2. Because the signal frequency is known together with the sampling speed and the number of samples the frequency component of the signals can

be estimated. The Fourier transform is calculated for the estimated frequency component and for two frequency components to the left and right of the estimated one. This is to find the dominant frequency component which has undergone a shift due to the irregular sampling frequency of the microcontroller. The maximum of the transform is compared to the previous one and is either stored or ignored. The process is then repeated for the other frequency components. The calibration of the phase shift follows and then the signal phasors are stored. Depending if amplification is sought the signals will be amplified, calibrated and stored. The impedance is then finally calculated by use of equation 4.10

4.3.4 Sampling Frequency Shifting Algorithm

This section is dedicated to the explanation of the programming that has gone into the protocol used to measure impedances over the spectrum of 100 Hz to 200 kHz. Special care had to be taken with regards to programming the protocol due to the small amount of memory that the microcontroller has. It can be seen that only a number of samples can be taken before the memory is full. The amount of samples that can be taken should stay constant over all measured frequencies as not to overload the memory of the microcontroller. This poses another problem. If one would have a set amount of samples that may be taken and one attempts to measure a low frequency signal with a high sampling frequency some information may become lost due to not sampling over the entire period of the signal. It was thus necessary to shift the sampling frequency as the frequency of the signal changes as to be able to measure the majority of the signals' period whilst still accommodating the limited memory of the microcontroller. Figure 4.3 demonstrates how this is done.

4.4 Chapter Summary

This chapter discussed the means by which signal analysis was used to calculate the body's impedance. Discrete Fourier analysis was incorporated together with additional algorithms to counter the limitations brought on by the digital hardware of the microcontroller. Calibration techniques were also implemented to calculate the impedance as well as to improve the accuracy of the measured impedance for higher frequencies.

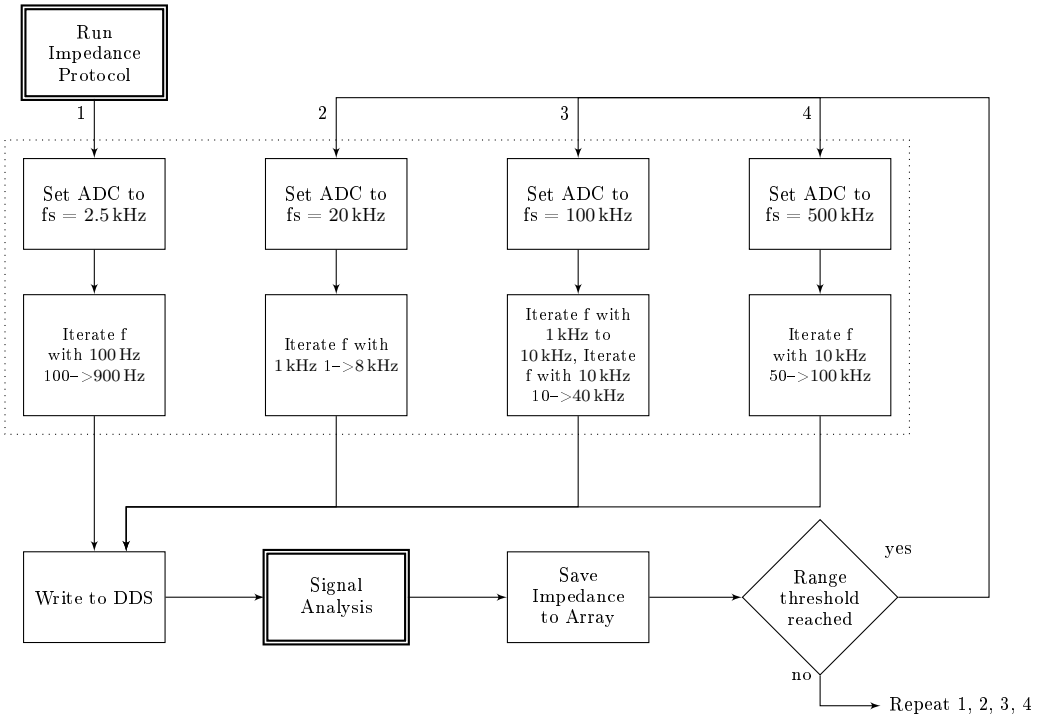

Figure 4.3: Flow diagram depicting frequency shifting to accommodate limited microcontroller memory

Chapter 5

Observations

This chapter is dedicated to the observations and validations of the different devices. It will strive to validate the efficacy of the devices as having the potential to measure hydration. In the case where the device's efficacy cannot be validated an explanation will follow with regards to the possible potential that the device has as a hydration sensor.

5.1 Impedance Accuracy and Validation

To test the efficacy of the impedance measuring devices a known circuit was constructed and measured four times. Figure 5.1 shows the magnitude and phase measurements of a parallel resistor and capacitor circuit. The resistor and capacitor in use is 28 kΩ and 270 pF respectively. The theoretical impedance and phase of the circuit is also given. As shown by Figure 5.1 the

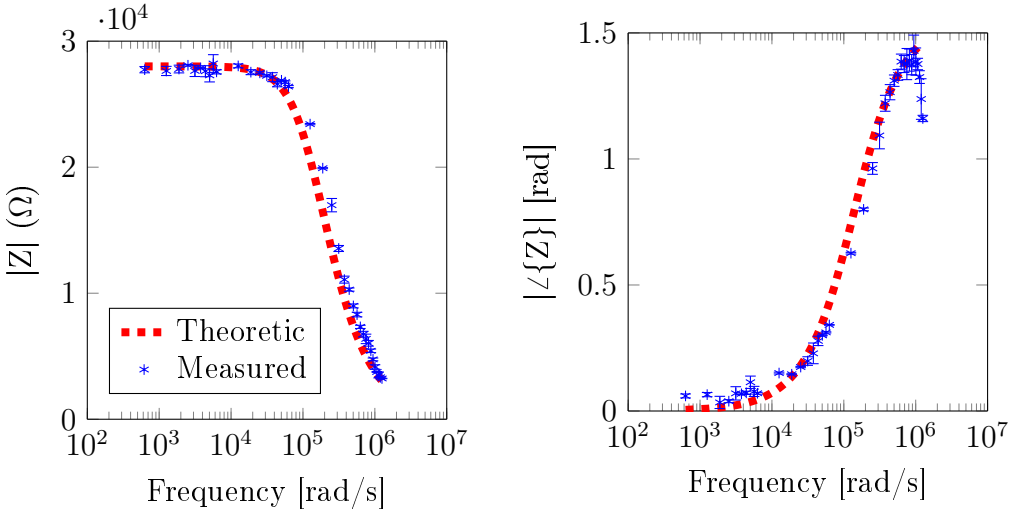

Figure 5.1: Magnitude and phase measurements of a parallel resistor and capacitance circuit

measured results follows the theoretical trend with little variance. Only the phase is subject to substantial error past the region of 100 kHz. The overall accuracy of the measured circuit boasted a good fit and is believed to be of sufficient quality to continue with the studies of this project.

5.2 BIA Observation

Numerous BIA measurements were taken from a single subject to investigate if the results will produce the Cole-Cole plot as mentioned in Chapter 2. The average ankle to ankle measurements are shown in Figure 5.2. The results do indeed show some form of curvature but according to Grimnes et al. and Jaffrin et al. the reactance should increase and the resistance decrease from lower frequencies up to around 50 kHz, and beyond that the reactance and resistance should decrease further forming the Cole-Cole plot [16, 36]. The measurements presented shows that the resistance and reactance decreases with frequency and does not increase to form the hill of the curve. The impedance is also far greater than that showed by literature [15, 36]. It is believed that this difference is caused by the small current of the BIA device. The device's peak allowable current is 20 µA under no load conditions and it could be that the current does not penetrate deep enough into the tissue and that the majority of the current travels through the skin.

Though Grimnes et al. and Foster et al. [36, 37] does state that bi-electrode configuration with a small current in the range of micro-amperes can produce the Cole-Cole plot, it is assumed that the reference resistor together with the added body impedance reduced the maximum current to the point where it cannot penetrate into deep tissue. Measurements will still be taken with the device even given the absence of the Cole-Cole plot as it is believed that the device can hopefully measure skin impedance which can be used as a marker for dehydration.

5.3 SC Observation

With the fabrication of the SC probe it is necessary to test its ability to measure hydration in the stratum corneum. This is done through a process inspired by the sorption-desorption test. The sorption-desorption test comprises of measuring the stratum corneum before and after the application of a water droplet and continuing measurements every 30 seconds [20]. The inspired test comprised of wetting a piece of cloth with warm water and draping it over the forearm, allowing the water vapour to be absorbed by the stratum corneum. This is done for 1 minute and afterwards for 5 minutes with measurements in between. Dry skin is used as a control and several measurements are taken at each instance. The results are displayed in Figure 5.3. As can be seen the

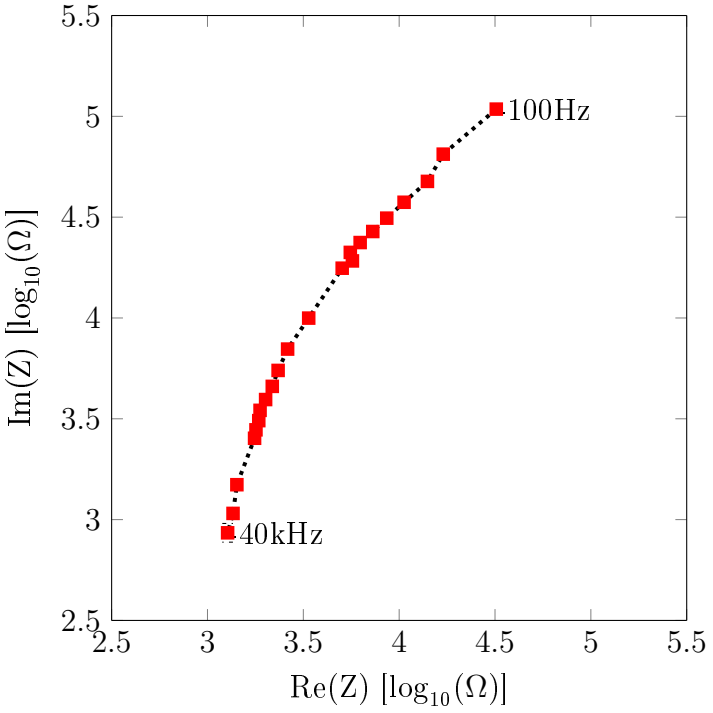

Figure 5.2: BIA ankle to ankle measurements on a single subject

base ten logarithmic of the resulting measurements shows a linear trend. The gradients of these trends remain constant between the different measurements with the elevation(y–intercept) of the trends decreasing. This is expected as water will improve conductivity of the stratum corneum. More interestingly is that there is a difference in measurements between the 1 minute and 5 minute tests showing that the device is able to measure different levels of water content in the stratum corneum.

5.4 IR Spectrometry Observation

The sorption-desorption test as done in the previous section is also implemented with the testing of the IR spectrometry device. It was mentioned in Section 2 that the absorption properties of the stratum corneum with its low water concentration are assumed to be negligible. The test done on it in this instance will elevate the water concentration beyond that of its natural concentration which is through TEWL. This also gives the opportunity to analyse how sensitive the device is to stratum corneum hydration as to assess its efficacy in the presence of accumulated sweat on the skin. Several measurements were taken and the results are shown in Figure 5.4.

The IR spectrometry measurements correlate with the theory in that the measured intensity declines with higher concentrations of water. The measured results show that the IR device can distinguish water content between the

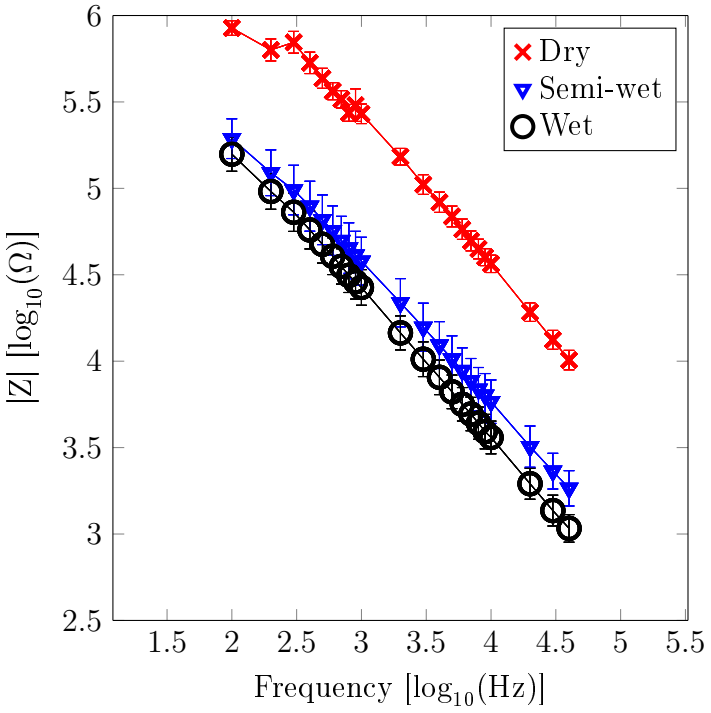

Figure 5.3: SC impedance results from hydration test performed on the stratum corneum for 1 minute and 5 minutes of exposure to water vapour

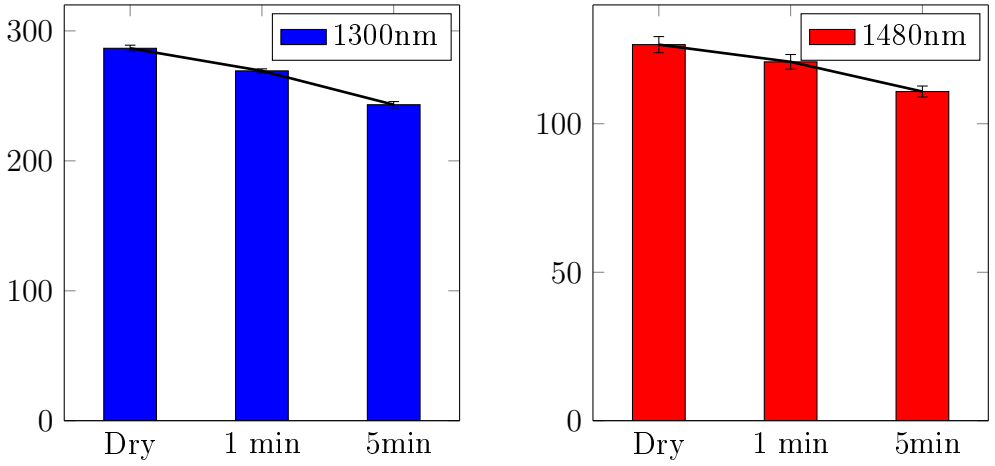

Figure 5.4: Infrared hydration test performed on the stratum corneum for 1 minute and 5 minutes of exposure to water vapour

different cases of stratum corneum hydration validating its ability to measure water content.

5.5 Chapter Summary

This chapter evaluated the validity and efficacy of the different devices by observing the trends of different tests. It is found that the BIA analysis does not follow the Cole-Cole plot as mentioned in Chapter 2 but does show some form of curvature. It is decided that the BIA device will still be used in the different studies as it might give a measure of hydration with regards to the hydrations state of the skin. The SC device and IR spectrometry devices were tested using a sorption-desorption inspired test where water vapour was absorbed by the stratum corneum to increase the water concentration therein. Both devices were able to measure the different levels of hydration in the stratum corneum proving their validity as hydration markers. With the validity of the devices known they will be implemented in the adult and infant studies as to ascertain their efficacy as human dehydration markers.

Chapter 6

Testing Methodology and Results

After researching, designing, fabricating and validating the devices, studies were conducted to asses the ability of the device's potential to work as dehydration assessors. Two studies were conducted: An adult study and an infant study. The adult study is set up to induce hypertonic hypovolemia in the subjects as to test the effectiveness of the different devices to work as an infield measuring tool for dehydration. The study also strived to prove that the devices have the potential to work on adults. The second study is one that includes infants that has succumbed to gastrointestinal distress causing the infants to be in a state of possible isotonic hypovolemia. Unfortunately for this study the BIA device is not included as ethical approval would not condone it. Here follows a description of the studies and later the results of said studies.

6.1 Standardized Testing and Validation Procedure

6.1.1 Ethical Approval

Prior to performing the adult and infant studies ethical approval had to be sought from the ethics committee of Stellenbosch. To receive approval for the studies one has to hand in a detailed document giving reason to why the study was necessary together with a thorough description as how the study will be carried out and in what sense can the devices pose a risk to those who will participate in the study. In addition to this document a letter of consent had to be made to be signed by all the subject that would participate in the study ensuring that they were well aware what was expected of them. The letter of consent and the letter of approval sent by the ethics committee can be found in Appendix C. The ethical application with regards to the adult study was handed in on December 2013 and was first denied by the committee. The application was reiterated and was later approved by the committee in

February 2014. The application for the infant study was denied twice before being accepted in September 2014.[1]

6.1.2 Adult Study

The procedure introduced in this section is closely related to that of Cheavront in "Biological variation and diagnostic of dehydration assessment markers" [27]. In his article he divided up the test period into two phases; phase 1 where euhydration (normal hydration) was achieved and phase two where dehydration methods were implemented to bring the subject to a state of dehydration. These phases are now described in detail.

Phase 1 It is necessary to bring the test subjects to a state of euhydration as this will form the basis against which all measurements will be compared to. To achieve this, subjects are asked to consume 3l of water in a period of 24 hours. One litre between waking up and 18:00 and two litres between 18:00 and 22:00. No food or drink is allowed between the times of 22:00 and 06:00. Euhydration measurements were then taken at 08:00. This is repeated for three days to obtain an average measure for the state of euhydration. In Cheuvront's study subjects were asked to follow a strict diet plan. It is assumed that this was done to eliminate possible hyper- or hypotonacity in the blood that could perturb measurements. For this study a strict diet plan was not prescribed as it was believed that with the number and nature of the test subjects confusion would ensue and would result in a waste of resources.

Besides the device measurements that were taken from the subjects the physical attributes of the subjects was also measured namely: blood pressure, temperature, heart rate and weight. Because weight is perceived to be the best measure for dehydration in a short period of time it was decided to use it as the base measurement for dehydration in the subjects. Blood was also drawn from the subjects to be sent away for osmolality analysis in the hope that this could be used as a second dehydration marker. Weight was given preference due to its simplicity and its swiftness of use.

Phase 2 In this phase dehydration is induced in the subjects through rigorous exercise routines. Subjects are asked to do three exercising sessions. Each session consisting of 50 minutes of exercise followed by a 20 minute break followed by physiological measurements and then device measurements. A break of 20 minutes is given in the hope that by the end of the physiological measurements the sweat on the subject's skin would have already evaporated. This

[1] This project was a cooperative attempt at building a viable hydration marker. One Eduard Kieser was responsible for the infant study and therefore the application with regards to the infant study is not appended to this document.

is done because it is believed that sweat could potentially perturb measurements. Subjects have a choice between cycling, rowing and jogging as a means of exercise. The intensity of the subjects' exercise is evaluated at certain intervals and it is strived to keep the intensity as close to 120 W as possible. The subjects are motivated to increase his/her intensity if it would seem that he/she is lagging. Though not all equipment implemented calorie counters the assessment was then based on the subject's respiratory harshness, visible sweat and overall exhaustion. The majority of the subjects for the study were diligent and exercised within satisfactory constraints.

After each session the subject's weight, heart rate, blood pressure and body temperature were measured followed by the device measurements. If the subject has succumbed to injury or has reached 4% weight loss due to dehydration they were removed from the day's study. After all subjects have completed their final session they were measured and their blood was drawn for serum osmolality analysis. Environmental conditions are also measured namely temperature and humidity to see if it had an effect on overall measurements.

Subjects received Energade and pizza after the final session to replenish fluids and electrolytes. The subjects were released when they felt well and rested. The responsibility of rehydration was left with the subject. The ethical application for this study can be found in the appendix of this document.

Shown in Figure 6.1 is a diagrammatic representation of the testing protocol.

6.1.3 Infant Study

In addition to the adult study an alternative study was conducted on infants. The premises for the study was Tygerberg hospital in the infant ward. Infants admitted to the hospital that had succumbed to dehydration were tested. Tests were done every four hours for the purpose of synchronizing with the rounds of the medical personnel. In addition to the device measurements the infants' weight and temperature were measured. Various factors were also measured namely: respiratory rate, heart rate and approximate intake of fluid. In addition to these measurements the practising physician was asked to complete a dehydration assessment of the infant whenever they did their rounds. The frequency of these assessments was subject to change as the practising physician would prioritize duties and the infant in question would be assessed at a later time.

As with the adult study, weight is used as the base marker for dehydration. Blood was not drawn for osmolality analysis as it was believed that ethical approval would not allow this.

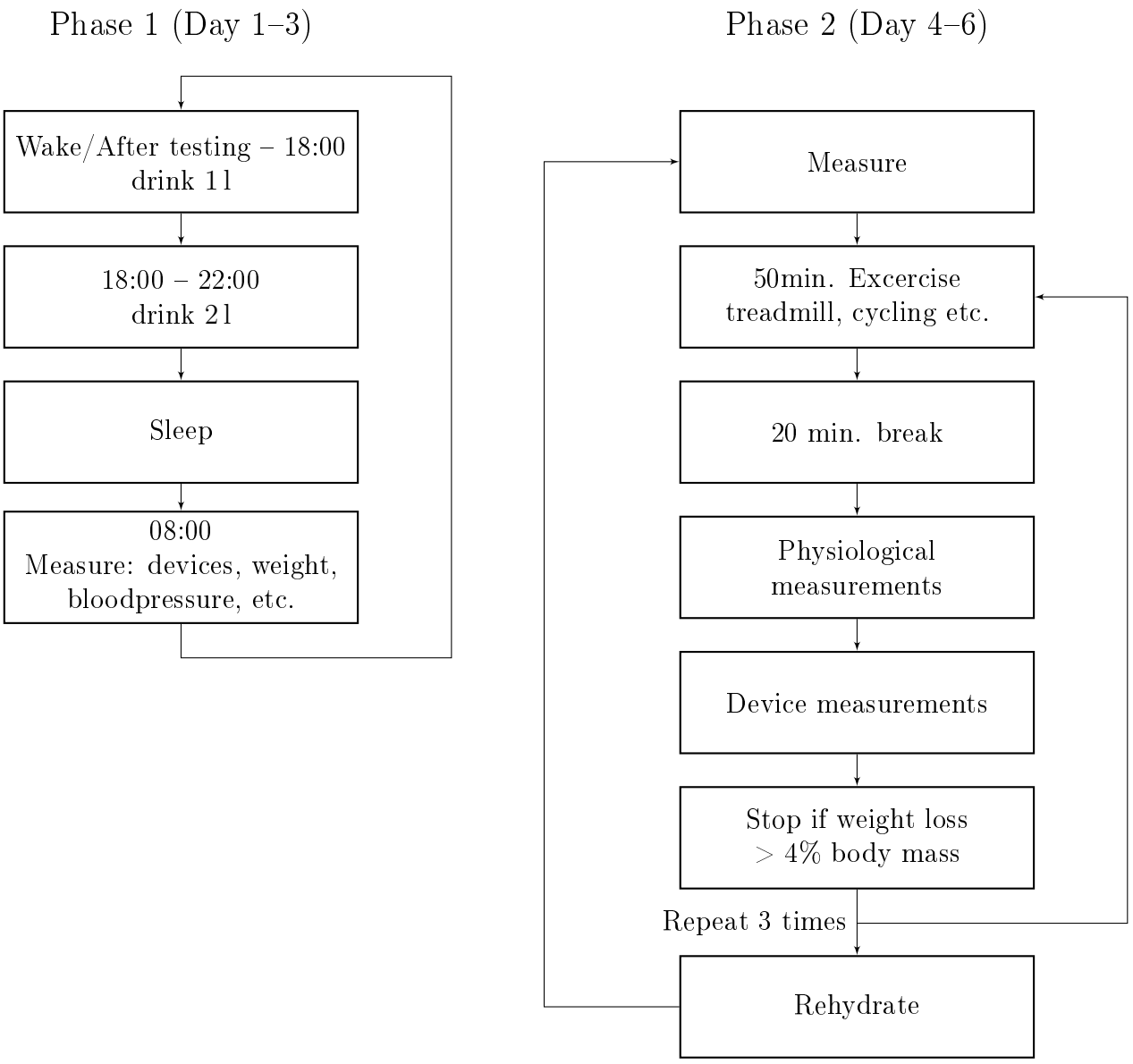

Figure 6.1: Adult testing protocol: Phase 1 and Phase 2

6.2 Results

6.2.1 Data Preparation

When performing BIA and SC impedance analysis on the subjects, one is presented with an array of impedances which needs to be analysed. It is necessary to incorporate methods to reduce the array to a single measurement which can be used for statistical analysis and to simplify the way the data can be presented.

Literature suggests that the resistance measured at low frequencies with regards to the BIA analysis will yield the resistance related to total body water and it is found that this resistance changes considerably with the onset of dehydration [15]. Literature showed this resistance can be extrapolated by using the Cole-Cole plot which is the fitted semicircle on the impedance data. This was discussed in Chapter 2. Though it is already shown in Chapter 5 that the desired impedance does not coincide with the Cole-Cole plot it is decided that the method will still be incorporated. As shown in the previous chapter the BIA measurements produced a circular curve. The same curve is observed in the adult subjects and it is decided that a circle will be fitted to the data and the circle coefficients will be used as single measured parameters for data analysis. It is decided that the maximum resistance of the curve will be used in the low frequency region as a measure for dehydration, as Röthlingshöfer showed that the larger affecting region of the Cole-Cole plot lies in the low frequency range associated with ECW. Once the resistance has been extracted from the data it is divided by the height of the subject in the hope of acquiring a normalised measure that is applicable to all subject given their anatomical differences.

It is observed in Chapter 5 that the base ten logarithmic of the SC impedance measurements yielded a linear line. It is observed that the line's gradient stayed constant whilst the intercept of the line reacted strongly with the onset of hydration in the stratum corneum. SC impedance measurements as measured in the different subjects yielded similar behaviour. The line intercept is thus used as a single measure for dehydration.

With the infrared results it is decided that the ratio of 1300 nm with regards to 1480 nm will be used as a single measure for dehydration. This is seen as a viable measure seeing that the two wavelengths exhibit different magnitudes of absorption and it is believed that with the lower absorption coefficient of the 1300 nm wavelength and its longer path length to the photodiode will cause the intensity of diffuse light to change drastically, faster than that of the 1480 nm wavelength causing the ratio to change forthwith. This change in intensity is demonstrated in Figure 5.4 in Chapter 5.

6.2.2 BIA Adult Results

Ankle to ankle impedance measurements were taken from nine adult subjects. Each subject was measured 15 times over the course of the study. The processed data, as described in Section 6.2.1 is grouped together and shown in Figure 6.2.

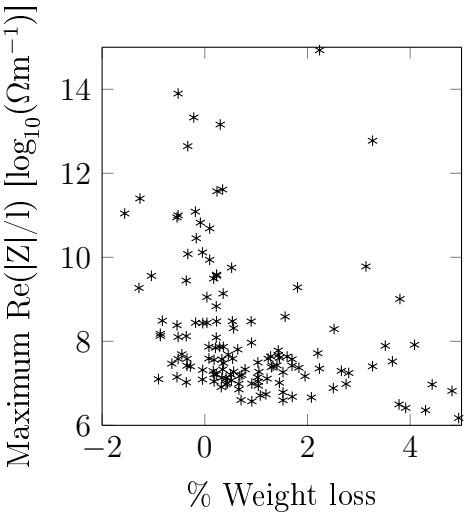

Figure 6.2: Grouped BIA results

Figure 6.3: Implementation of the BIA device.

Results yielded a scattered behaviour with no distinguishable trend. Take note of the measurements taken at high levels of dehydration and compare it with those closer to euhydrated state. It can be seen that the data near to higher levels of dehydration is clustered at a resistance lower than that measured in the euhydrated state. This does not coincide with the theory as

shown by Röthlingshöfer et al. [15] who showed that the real impedance will increase with dehydration.

6.2.3 SC Adult Results

The results obtained via the SC measurements are depicted in Figure 6.4. The data shown is the grouped data of the nine adult subjects whom competed in the study. Measurements were taken from the dorsal side of the forearm. Once

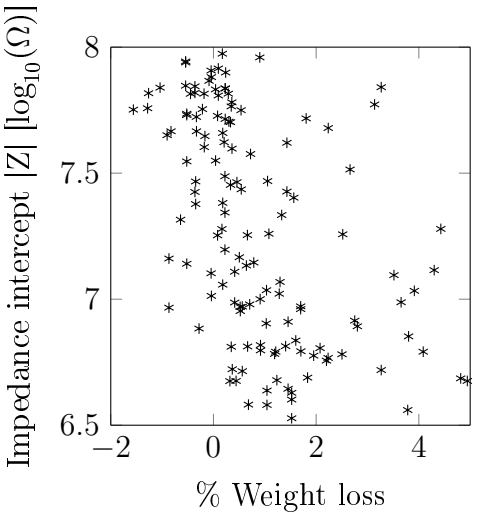

Figure 6.4: Grouped stratum corneum results

again the data provided is scattered and no distinguishable trend can be seen. The results do not agree with the theory as the impedance is declining with increasing levels of dehydration. It was expected that the impedance would increase as was observed in Chapter 5.

6.2.4 IR Adult Results

Figure 6.6 displays the grouped IR measurements from the nine subjects of the adult study. Measurements were taken from the dorsal side of the right forearm. The presented data shows no distinguishable trend and measurements decline with higher levels of dehydration. This does not coincide with the theory as high intensity measurements are expected with high levels of dehydration due to fewer absorbing chromophores in the skin.

Figure 6.5: Implementation of the SC device.

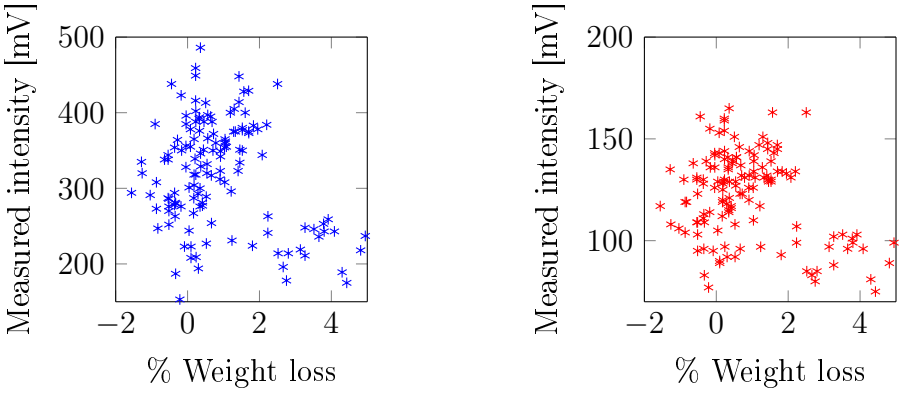

Grouped 1300 nm results Grouped 1480 nm results

Figure 6.6: Grouped adult infrared results

6.2.5 Adult Discussion

For the sake of interest a linear regression analysis was performed on the data as to investigate the significance of the different variables. The information retrieved from this analysis is shown in Table 6.1.

Linear regression attempts to fit a linear model namely

$$y = ax_1 + bx_2 + cx_3 \tag{6.1}$$

to the data (weight loss), given the different variables, namely the BIA measurements, SC measurements and IR measurements. Linear regression derives the coefficients of these variables which can be used to estimate the weight loss given any set of measurements. The estimated coefficients of the variables are given in the "Estimate" column of Table 6.1. The "SE" column gives the standard deviation of the estimated coefficients and can be divided into the

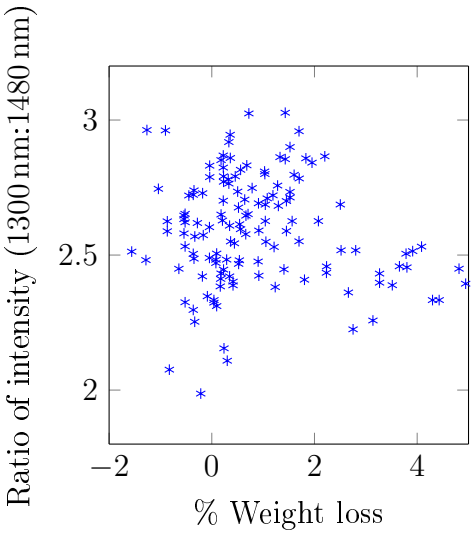

Figure 6.7: Adult grouped measurements shown as IR (1300 nm:1480 nm) ratio

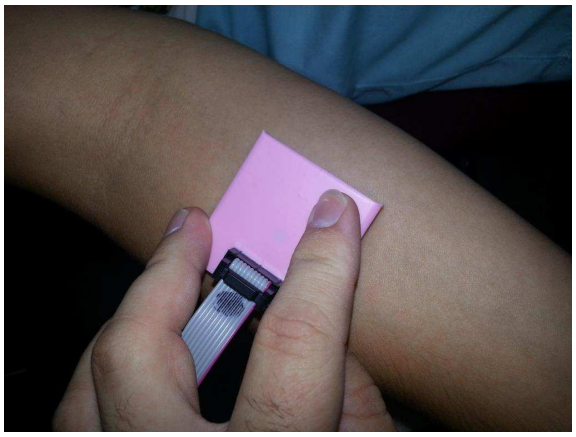

Figure 6.8: Implementation of the IR spectrometry device.

estimated coefficient to give the tStat value which is used to derive the p-value. The SE value gives to some extent the precision of the model's coefficient in predicting weight loss. The SE value will not be used to determine the model's efficacy. The p-value will be used which gives the significance of each coefficient with regards to the estimated weight loss. A variable with a p-value larger than 0.05 is considered to be significant.

The linear regression analysis from Table 6.1 shows that the SC and IR measurements have high significance ($p<0.05$) whereas the BIA measurements are less significant. This implies that with changes in SC and IR measurements a change was also observed in the weight loss of the subject. This is strange as it has already been mentioned that the measurements do not coincide with the theory and yet linear regression has shown that two of the

	Estimate	SE	tStat	pValue
intercept	0.1671	0.022968	7.2753	2.8301×10^{-11}
BIA	-0.00073098	0.00079041	-0.92482	0.35676
SC	-0.014967	0.0028611	-5.2312	6.4966×10^{-7}
IR	-0.016822	0.0052378	-3.2116	0.0016611

$R^2 = 0.299$, Model pValue $= 3.91 \times 10^{-10}$

Table 6.1: Linear regression analysis of the measured variables: BIA, SC and IR

variables are significant for the prediction of percentage weight loss. Furthermore the p-value for the model itself is smaller than 0.05 and thus the model is significant given the observable variables. It is thus possible that the devices are measuring something else that changes linearly with the weight loss of the subjects. It is assumed that this perturbing factor is sweat. Though time was given for sweat to evaporate it did not and this could be attributed to the fact that the studies were done indoors during winter. The cold weather together with the high humidity and absence of wind flow resulted in the sweat accumulating on the skin which was absorbed by the stratum corneum. This is clearly revealed by the stratum corneum measurements which decreased with dehydration where observations show that it should be increasing. This could also have perturbed the measurements of the BIA device as its resistance also declined with higher levels of dehydration. With regards to the IR device there are two possible perturbing factors, of which one is sweat. The other could be due to heterogeneity of the skin on the arm resulting in the data being so wide spread.

It should also be noted that only two of the subjects were able to dehydrate themselves beyond 2%. It is stated by Cheavront [10] that the body regulates the plasma concentration of the blood and only shows a change in osmolality beyond 2% weight loss due to water loss [10]. This could have influence measurements as only two of the nine subjects could achieve this state of dehydration, diminishing statistical relevance.

The devices of this project were implemented in an adult study to confirm if it is possible to assess real time dehydration in people. Unfortunately a perturbing factor was present in the studies and it is believed to be sweat caused by strenuous exercise. It is believed that the sweat accumulated on the skin and was absorbed before it had a chance to evaporate. It can therefore be assumed that the devices fabricated in this project are not suited for infield measurements with regards to active adults. This does not disprove the ability of the device to measure dehydration. It is very likely that the device can measure dehydration given a standard testing environment with controlled humidity, temperature etc. or given that certain prerequisites are met, for example measuring in a temperature that does not cause sweating.

6.2.6 Plasma Osmolality

As an added marker a few samples of blood were taken from the subjects and sent away for osmolality analysis. Upon receiving the analysis a linear regression analysis was done to see if the devices could pick up on plasma changes in the subjects. The plasma osmolality results are depicted in Figure 6.9 and is shown in Table 6.2.

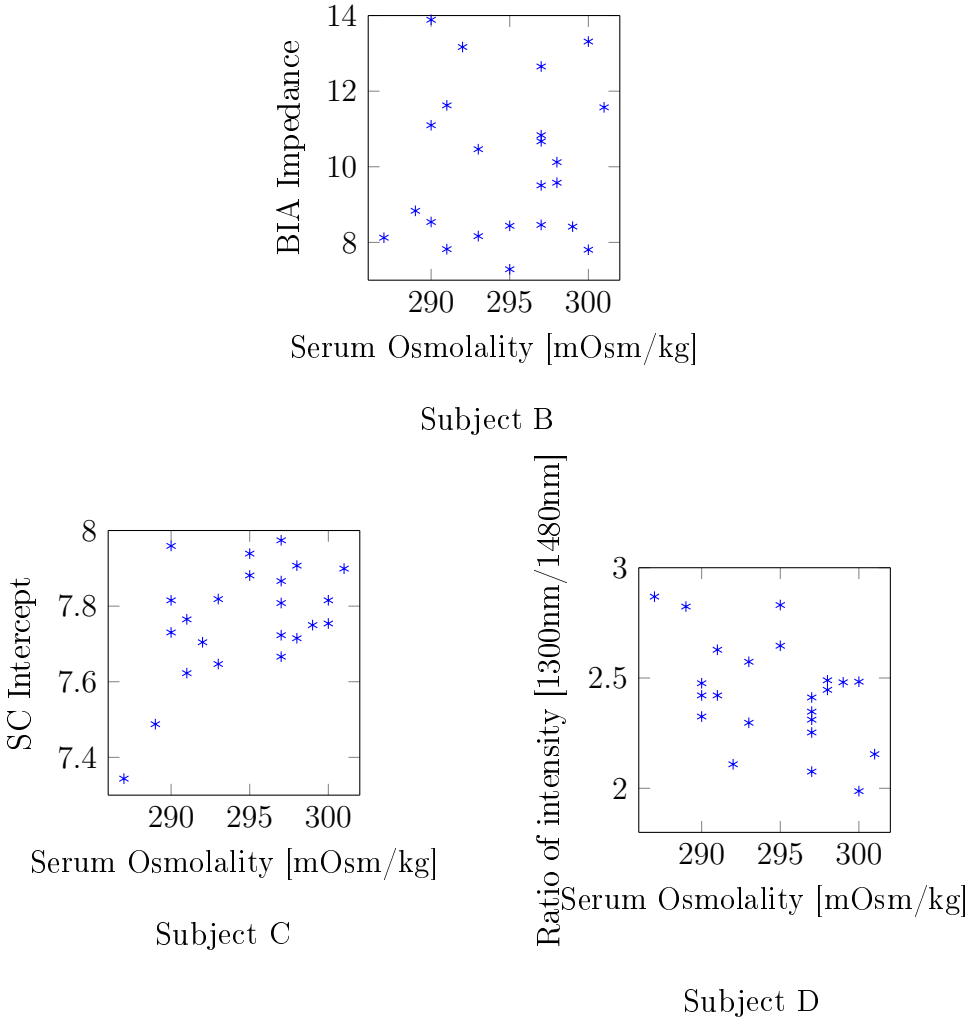

Figure 6.9: Plasma osmolality analysis from the adult study

From the linear regression analysis it can be seen that none of the measured variables have a p-value smaller than 0.05 with the exception of the IR measurements. This implies that the BIA and SC variables are not significant in predicting the plasma concentration of the blood, however the IR device might be able to. If one were to investigate the estimated coefficient for the IR device, one would see that it has a negative gradient implying that with higher levels of IR ratio, as expected with dehydration, the osmolality will decline.

	Estimate	SE	tStat	pValue
intercept	256.71	45.507	5.6411	1.9388^{-5}
BIA	-0.664	0.47373	-1.4016	0.17715
SC	8.9303	5.0466	1.7696	0.092848
IR Spec.	-10.191	4.1761	-2.4404	0.024638

Table 6.2: Linear regression analysis of BIA, SC and IR variables with regards to plasma osmolality

Osmolality increases with the onset of dehydration debunking the validity of the IR device. It is believed that the sweat factor as mentioned in the previous section influenced the IR measurement into providing a small p-value. This concludes that the different devices are incapable of measuring plasma concentration given the environment used in the study.

6.2.7 Infrared Spectrometry Infant

It is aimed in this project to include infant studies to investigate if the proposed devices can measure an infant's hydration levels. Unfortunately due to difficulties with ethical approval the study was conducted near the end of the project deadline. In addition to this the number of subjects were few as the study could only be conducted outside of the time period when the onset of dehydration is highest in infants due to diarrhoea. This resulted in only four subjects being measured during the study and though few this section will strive to analyse and interpret the data in an attempt to find promising aspects that could be used for future work.

Given in Figure 6.10 are the measured IR results of the four subjects. All measurements where taken on the subjects' stomach. Note that the 1300 nm and 1480 nm are given on the same plot and their axis are on the left and right of the graph respectively.

The data gives an indication that high levels of intensity are expected with the onset of dehydration. Noticeably these results tend to decline over the rehydrated weights of the subjects to the point, close to euhydrated state, where the measurements increase again. This is only the case for subject A,C and D, however subject B was measured with longer periods of waiting times and the detailed measurements between 4% and 0% of weight loss, where one can see this occurrence, is unknown. Attention should be given to the measurements taken at the higher levels of dehydration and it should be noticed how the measurements are significantly high in comparison to the rest of the measurements. This is discussed further in the discussion section.

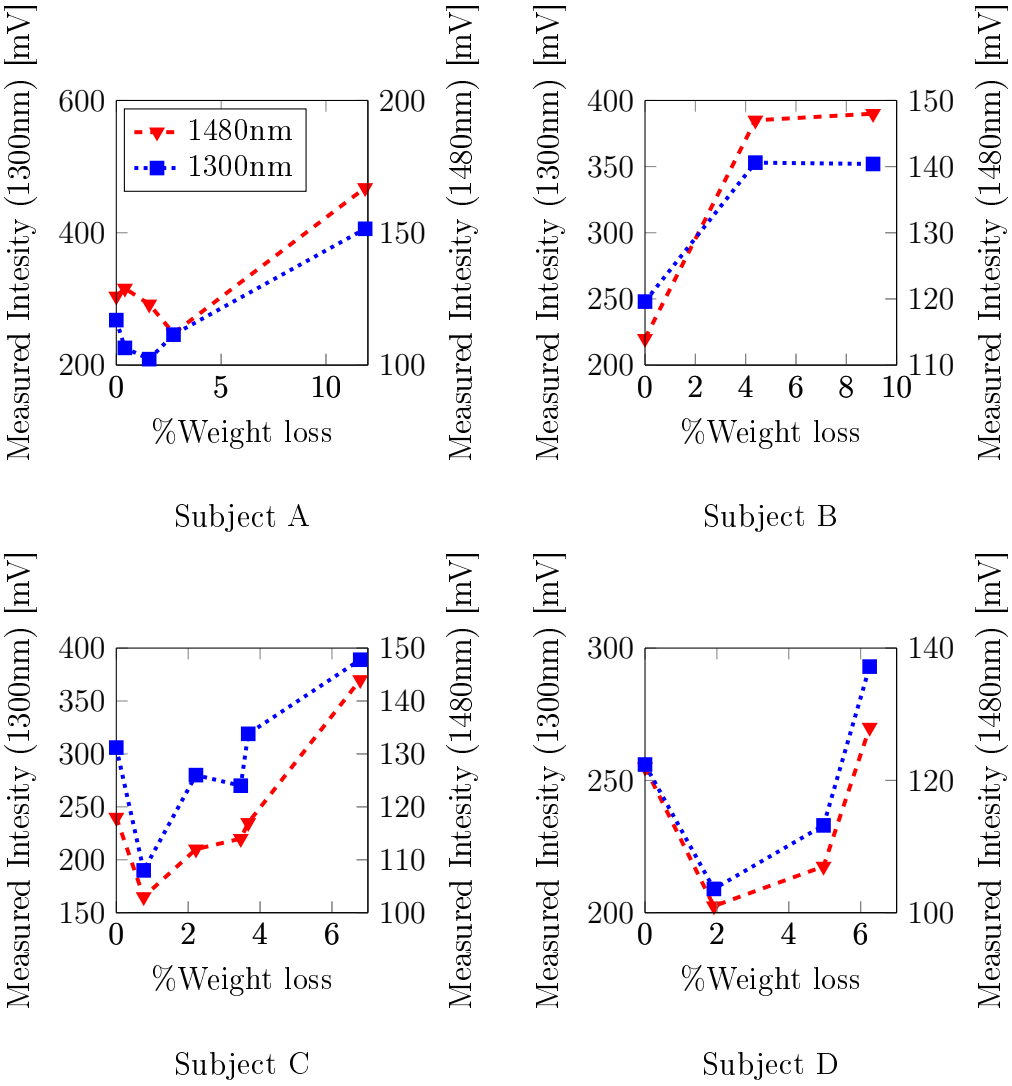

Figure 6.10: Infrared spectrometry observations of four infant subjects

6.2.8 Infrared Spectrometry Infant: Discussion

As mentioned the intensity levels of the measurements tended to decline with an onset of water weight up to the point of around 4% weight loss due to water loss. This coincides with the theory which dictates that with the rise of water concentration the number of infrared absorbing chromophores increases as well and vice versa. With a large number of chromophores the measured intensity will decrease whereas with a small number of chromophores the intesity will increase. The observed behaviour could be an indication of the blood flow to the skin that was first restricted, via vasoconstriction, when the subject was dehydrated and is now slowly returning, via vasodilation, increasing blood flow and therefore blood volume while the subject is rehydrating. The measurements taken in the range of 0% and 4% weight loss do not coincide with the

mentioned theory. This could be due to the altered morphology of the skin and blood cells. Friebel et al. [24] showed that the optical properties of blood can change and it can be due to a number of reasons namely bloodflow, pathlength of blood cells etc. It can be assumed that when rehydrating the blood cells become engorged with water altering the pathlength of the infrared light, apart from this blood flow is now present in the skin where it was not before. This all could attribute to the dynamics of measurements taken in the 0% to 4% range.

The results of the infrared spectrometry measurements as discussed in this section is promising, however the amount of data which was accumulated for the study is insufficient to prove, irrefutably, that the theory coincides with the measurements and that IR spectrometry can be used as a marker for dehydration. Given this, IR spectrometry as a marker for dehydration cannot be ignored as it could give a possible measure for isotonic hypovolemia and/or hypertonic hypovolemia in vivo. The results that have been displayed, though not enough to give proof, is a viable observation to motivate further study.

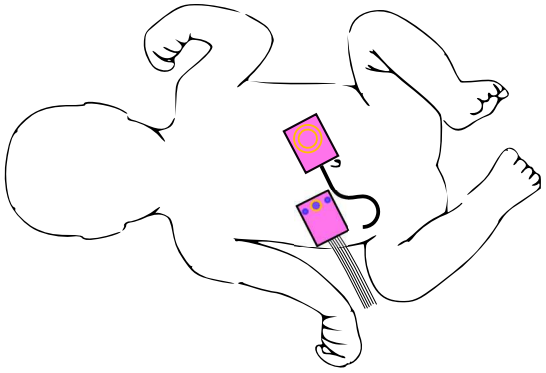

Figure 6.11: Illustrated implementation of the SC and IR spectrometry devices on an infant.

6.2.9 Stratum Corneum Infant

In was observed in Chapter 5 that with the onset of water on the stratum corneum it will absorb the water and the measured impedance of the stratum corneum will decrease significantly. It was found that the trend of the base ten logarithmic of the curve was linear and that the gradient of said curve would stay constant with the different degrees of water content. The stratum corneum impedance measurements produced by the infant subjects were similar to that in the observation and the adult studies and as with the adult study the intercept of the fitted line was used as a measure for dehydration. This was plotted against the weight loss due to water loss and is shown in Figure 6.12.

The measured results are inconsistent and do not follow any obvious trend.

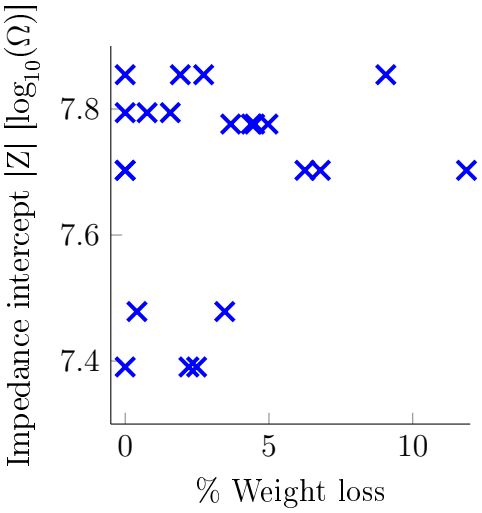

Figure 6.12: Grouped infant stratum corneum results

6.2.10 Stratum Corneum Infant: Discussion

Not many conclusions can be derived from the measured data. It was thought that under individual investigation of the subjects that a measured trend can be found as was found with the infrared device. This is not the case as no information could be found that could even lead to an observation. Two of the subjects did however produce results that correlated with the observation. It was not seen as applicable to display these results as it was discussed in Section 6.2.5 that the SC device measurements are subject to sweat and possibly humidity and it was assumed that the same perturbing factors had the same effect on the measurements.

The stratum corneum probe though mentioned by many sources as a means to measure stratum corneum hydration is not an effective device for the measuring of overall hydration with regards to the infant study. This can be due to the non-standard setting of the study. Temperature, humidity etc. was not controlled and could have contributed to the perturbed measurements of the infants. The device might be able to measure dehydration but it is believed that this will not be possible in a non-standardised setting.

6.3 Chapter Summary

This chapter reviewed the results from both the adult and infant studies and discussed the nature of the results including the possible perturbing factors present in the study with each device. Both studies did not yield auspicious results, it did however produce results motivating the use of IR spectrometry for the measurement of dehydration in infants. The quantitative assessment of dehydration still remains an ever elusive standard.

Chapter 7

Conclusion and Future Work

7.1 Conclusion

This thesis strives to investigate the applicability of different devices as dehydration markers suitable for both infants and adults. Bioelectrical impedance analysis, stratum corneum impedance analysis and infrared spectrometry were implemented in this endeavour to find a golden standard for dehydration.

Literature was provided showing that these markers are not conventionally used for measuring dehydration. Only one literature source was found [15] regarding the use of BIA as an hydration marker and no explicit sources could be found for the use of the SC measuring device or the IR spectrometry being used as a marker for dehydration. It was explained in the literature study why these three devices could be used as markers for dehydration. The BIA device having the ability to measure extracellular water in the body, the ability of the stratum corneum device to measure transepidermal water loss and the IR spectrometry device possibly having the ability to derive the water or plasma concentration in the skin.

Various techniques were incorporated to develop the needed circuitry and computer programming to design and fabricate the devices. Signal analysis was implemented to calculate the gain and phases of the different signals to calculate the impedances of the body. All signal analysis was done on the microcontroller to prove that portability is possible with the three different devices. This was indeed possible and a computer was only used to sort and store the accumulated data. Circuitry was developed to buffer and amplify the signals measured. Fortunately the measured signals were large enough and the amplifiers were not necessary. A GUI was programmed as a way to ensure data quality assurance and to catalogue the data under each subject the study was performed on.

Observations were made to test the validity of the devices and showed that two of the devices did coincide with the theory and produced results that showed that it can pick up on hydration levels in the stratum corneum. This

observation was done through exposing the stratum corneum to water vapour allowing it to absorb the water and retain it. Several measurements were taken with the IR spectrometry device and the stratum corneum impedance device and the results showed that the devices could indeed differentiate between dry skin, semi-wet skin and wet skin. The BIA was validated through comparing the measurements with that found in literature. The results did not form the Cole-Cole plot as mentioned by literature and it is believed that this is due to the low current of the device causing the device to not be able to measure in deep tissue. The BIA analysis was however still kept in the study as it was believed that it could still give results regarding the hydration state of the skin.

Two studies were conducted during the course of the project. A study on adults who were subjected to strenuous exercise to induce hypertonic hypovolemia and an infant test where the infants included in the study are those that have succumbed to gastrointestinal distress inducing isotonic hypovolemia in the infants. Nine subjects participated in the adult study and the results from this study did not show a trend in measurements. It was later assumed that the measurements were perturbed by sweat showing that the devices may not be suitable as an infield measurement tool with regards to measuring hydration in tandem with active lifestyle practises. The infant study yielded results for four subjects and though not many certain observations could be made with regards to the infants, there lies promise in using IR spectrometry as a method for investigating the effects of isotonic hypovolemia and possibly hypertonic hypovolemia. Though no hard evidence can be given towards the effectiveness of IR spectrometry as a hydration marker it shows that the method cannot be ignored and could be an inexpensive method for measuring dehydration.

7.2 Future Work

Many challenges were encountered in this project. This section is dedicated to those who wish to continue the work related to this project. Here follows the challenges that were encountered and the means by which the next iteration of the project can be improved.

7.2.1 Hardware and Design

7.2.1.1 Microprocessor

Many difficulties were encountered with the choice of microcontroller. The Arduino UNO32 is capable of a sample speed that makes it possible to measure frequencies of close to 200 kHz. However as mentioned in Chapter 4 the process of sampling is sequential and the sampling speed is subject to change. It is difficult to find a microcontroller with a fast enough clock speed to do the same as the UNO32 but the last mentioned characteristics are detrimental to the

performance and the accuracy of the measured signals. It is advised that the following iteration of the device incorporate independent ADC IC's with their own independent clock or that the microcontroller not be programmed using the arduino environment and rather the PIC32 environment. This is to ensure that the performance of the microcontroller does not influence the sampling of the signals. These IC's can be coupled in parallel with the microcontroller to ensure a fast transmission rate.

7.2.1.2 Sampling Methods

To ensure that the device remains portable it was necessary to only have a set amount of samples as to ensure that the microcontrollers memory does not become saturated. To ensure the integrity of the data it was necessary to constantly change the sampling speed with the different frequency rates of the signal. This can be avoided by generating an additional signal close to the frequency of the inducing signal using a second AD9850 DDS module. This signal can be used to mix the measured signals to a lower frequency and depending on how accurately the signals can be generated all signals can be mixed down to the same frequency. This makes it possible to use a single filter for the entire spectrum of signals. Once measured the original signals can be extracted through signal techniques.

7.2.1.3 Digital Interface

It was thought that coupling the microcontroller via a WIFI connection to a GUI on the computer would be productive and ensure data integrity. Though this is true this was also counterintuitive as it was a laborious struggle to transport a laptop, the devices and a router. In future work where studies should be completed it is advised to keep the device as simple as possible and to incorporate onboard data storage, for example using an SD card. In the case where wireless transmission is needed and unavoidable, preference should be given to Bluetooth technologies which will be a more favourable option given its simplicity and the fact that it does not require a router.

7.2.1.4 WIFI

Weigh the different options for establishing communication between a portable device and a PC as the decision could define the complexity of the device's usability. A great struggle was encountered by using the MRF24WG0MA WIFI module which was frustrating and pilfered a large amount of time that could have been spent better. The WIFI module that was used for the project was dated and had very little support from the providing company. In addition to this a router was necessary to establish a connection as the module did not have ad hoc functionality. The protocol used by the module was also selective as it could only connect to some routers. It would have been far easier to

have used a Bluetooth module as no 3rd party device (e.g. a router) would be needed to establish a connection to a laptop.

7.2.1.5 Infrared Spectrometry

Manufacturers of infrared diodes were researched and a manufacturer was found that provided affordable diodes and photodiodes. The only problem was that the manufacturers took four months to manufacture the components resulting in a delayed schedule. The only advice that can be left here is that cost should not dictate one's decision on parts, but rather time. Had the components been ordered from a different vendor they would have arrived two weeks after placing the order.

7.2.2 Research

Hydration was investigated by measuring with only two wavelengths as this was a cost-effective investigation to see if hydration can be measured using infrared light. Though positive results were shown it would be interesting to investigate dehydration by measuring several wavelengths in the spectrum as the curvature of the intensities could give more insight to the hydration well-being of the subject.

If the one would endeavour to implement BIA as a hydration marker, it is advised that a current source is incorporated and that the source is not subject to change and has some form of control feedback keeping the output constant. It is further advised that the source be at least 1 mA. Though no reviewed literature could be found that recommends this current some sources have mentioned it.

BIA is an already widely used method for estimating the body's composition and unfortunately only one source could be found that suggests that BIA can be used to indicate dehydration [15]. It would thus be of great contribution if this field of research can be expanded with regards to BIA being a capable hydration marker.

It was strived in this project to manufacture three different devices each originating from a different field of biomedical engineering. It goes without saying that each field is widely diverse having extensive information and theories on their relevant subjects. Each of these devices could have been on its own a masters project and what has been shown in this report is but an overview of the different fields. If there be someone that would continue with this work let it be with one of these three devices as an in-depth investigation into the single device could yield more favourable results.

Appendices

Appendix A

Printed Circuit Boards

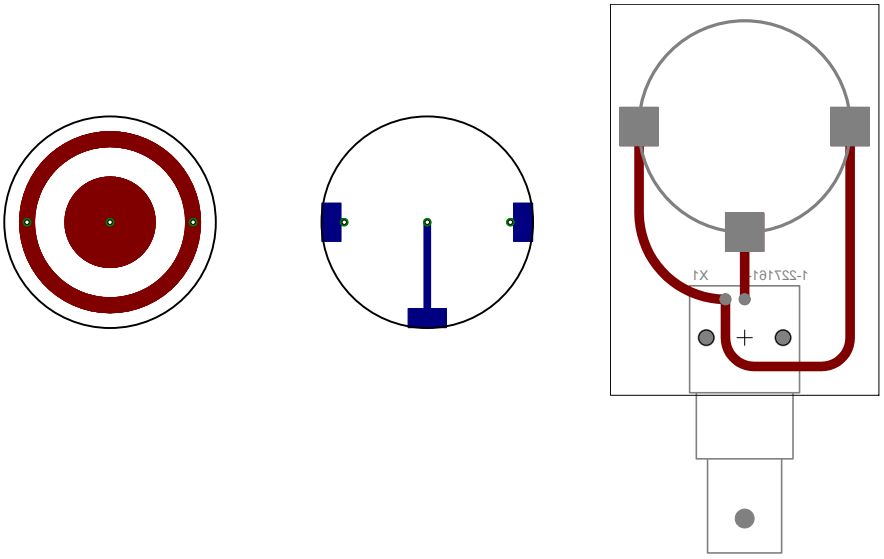

Figure A.1: Stratum corneum circuit configuration
From left to right: The stratum corneum probe top layer as seen from above, probe bottom layer seen from above and the probe housing.

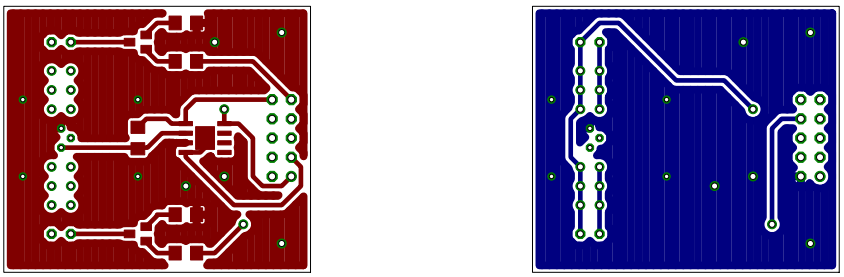

Figure A.2: Top and bottom layer of IR pcb circuitry

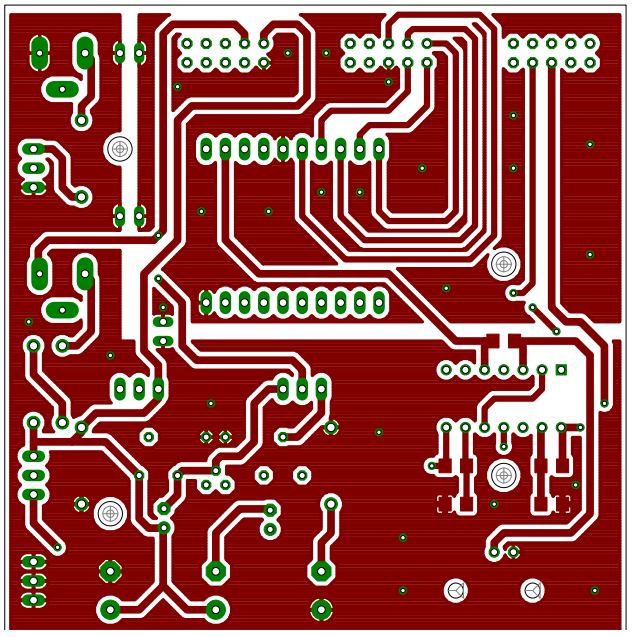

Figure A.3: Rail splitter, amplifier, buffer and DDS pcb top layer

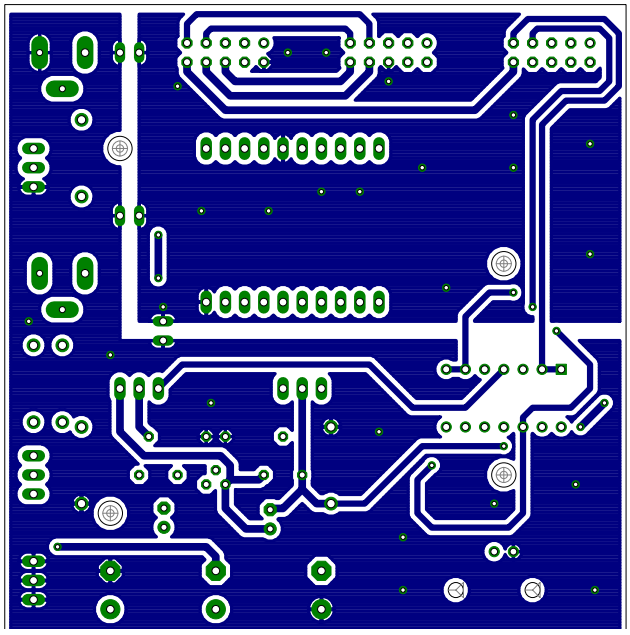

Figure A.4: Rail splitter, amplifier, buffer and DDS pcb bottom layer

Appendix B

Monte Carlo Simulation

Photon transport and absorption can be simulated using the Monte Carlo method. This consists of generating a photon and then making it undergo a random walk in a medium. The photon will undergo scattering and will also lose some of its energy due to the absorption properties of the medium. It was sought to implement the Monte Carlo simulation in this project but the time needed to construct a heterogeneous medium to mimic skin would have been a laborious task that would have pilfered too much time from the project. A homogeneous medium that mimics the air to skin optical behaviour was simulated and is shown in Figure B.1 and B.2. It was later decided that these simulations will only be used as an observation as the results from a homogeneous medium simulation would give vague results that cannot be used as a comparable medium for the practical measured results.

[29].

For clarity the fluence rate as observed at the boundary is shown in Figure B.3. As can be seen from all the different figures the 1480 nm IR light is quickly absorbed near the excitation point and the fluence rate decreases faster than the fluence rate of the 1300 nm IR light. This is expected seeing that the 1480 nm light has a higher absorption coefficient than the 1300 nm light. As mentioned these simulation were done as an observation to investigate the behaviour of photons given the two different wavelengths and their different optical properties. The simulations confirmed the difference in absorption and movements and spurred on the fabrication of the IR devices.

The optical properties of the mediums were taken from Bashkatov et al.[34]. The code used for the Monte Carlo simulation is the creation of Prof. Steven Jacques and has been used with his permission

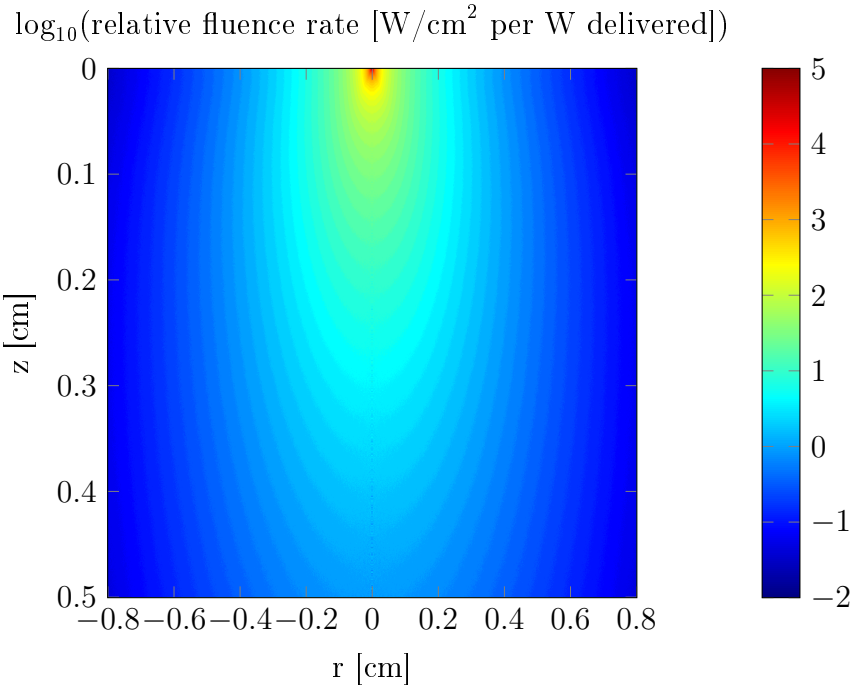

Figure B.1: Fluence rate observed in a homogeneous semi-infinite medium subjected to a point source of 1300 nm of IR light

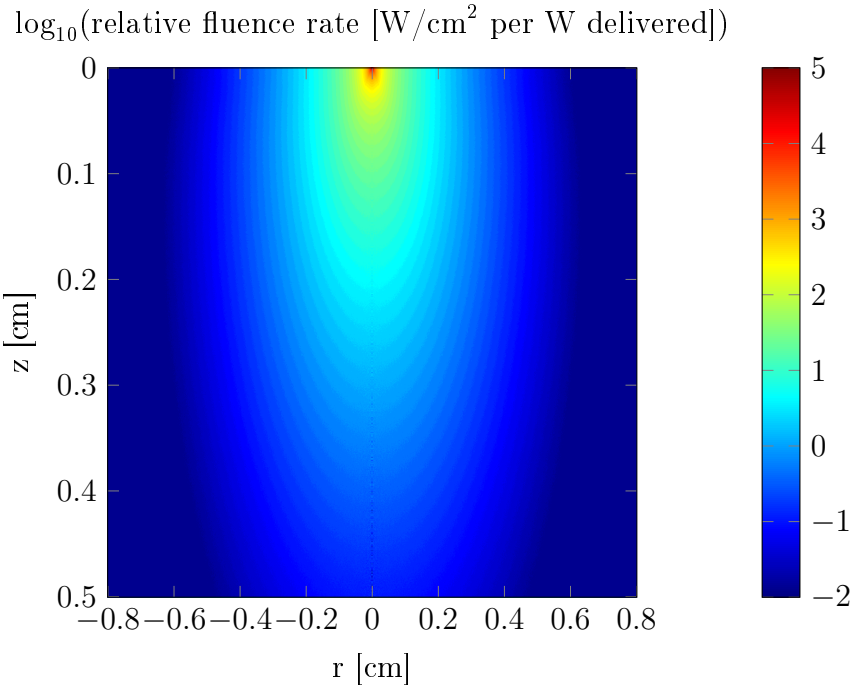

Figure B.2: Fluence rate observed in a homogeneous semi-infinite medium subjected to a point source of 1480 nm of IR light

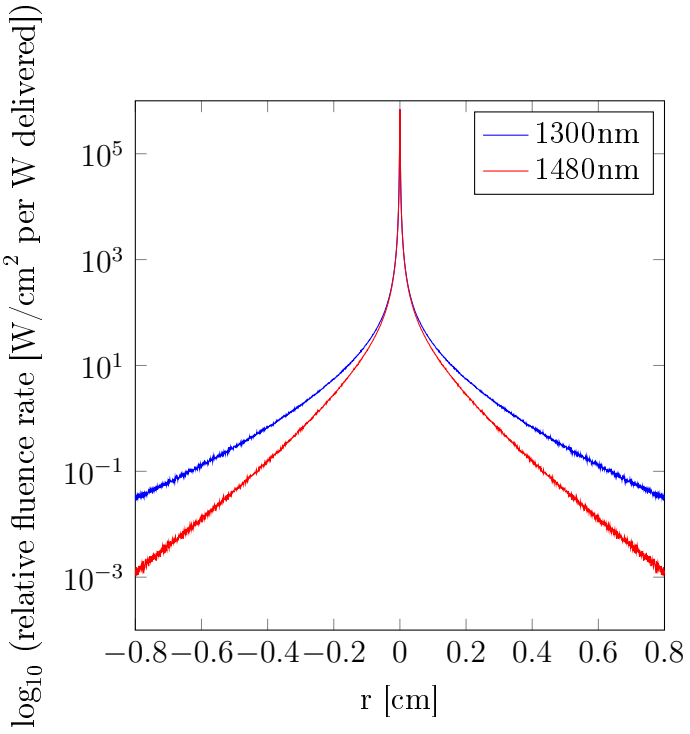

Figure B.3: Fluence rate observed at the boundary of the air and medium subjected to 1300 nm and 1480 nm of IR light

Appendix C

Ethical Approval

UNIVERSITEIT·STELLENBOSCH·UNIVERSITY
jou kennisvennoot • your knowledge partner

Approval Notice

New Application

25-Feb-2014
Scheffer, Cornelius C

Ethics Reference #: S13/10/204
Title: Quantitative Hydration Sensor Development (Adult Testing)

DearProfessor Cornelius Scheffer,

The **New Application** received on **12-Nov-2013**, was reviewed by members of **Health Research Ethics Committee 1** via Minimal Risk Review procedures on **25-Feb-2014** and was approved.
Please note the following information about your approved research protocol:

Protocol Approval Period: **25-Feb-2014 -25-Feb-2015**

Please remember to use your **protocol number** **(S13/10/204)** on any documents or correspondence with the HREC concerning your research protocol.

Please note that the HREC has the prerogative and authority to ask further questions, seek additional information, require further modifications, or monitor the conduct of your research and the consent process.

After Ethical Review:
Please note a template of the progress report is obtainable on www.sun.ac.za/rds and should be submitted to the Committee before the year has expired.
The Committee will then consider the continuation of the project for a further year (if necessary). Annually a number of projects may be selected randomly for an external audit.
Translation of the consent document to the language applicable to the study participants should be submitted.

Federal Wide Assurance Number: 00001372
Institutional Review Board (IRB) Number: IRB0005239

The Health Research Ethics Committee complies with the SA National Health Act No.61 2003 as it pertains to health research and the United States Code of Federal Regulations Title 45 Part 46. This committee abides by the ethical norms and principles for research, established by the Declaration of Helsinki, the South African Medical Research Council Guidelines as well as the Guidelines for Ethical Research: Principles Structures and Processes 2004 (Department of Health).

Provincial and City of Cape Town Approval

Please note that for research at a primary or secondary healthcare facility permission must still be obtained from the relevant authorities (Western Cape Department of Health and/or City Health) to conduct the research as stated in the protocol. Contact persons are Ms Claudette Abrahams at Western Cape Department of Health (healthres@pgwc.gov.za Tel: +27 21 483 9907) and Dr Helene Visser at City Health (Helene.Visser@capetown.gov.za Tel: +27 21 400 3981). Research that will be conducted at any tertiary academic institution requires approval from the relevant hospital manager. Ethics approval is required BEFORE approval can be obtained from these health authorities.

We wish you the best as you conduct your research.
For standard HREC forms and documents please visit: www.sun.ac.za/rds

If you have any questions or need further assistance, please contact the HREC office at 0219389156.

Included Documents:
Consent Forms
Declaration - Kieser
Synopsis
Declaration - Smith

Cover letter
CV - Blanckenberg
Protocol
Checklist
Declaration - Blanckenberg
CV - Kieser
Application Form
CV - Smith
Declaration - Visser
Supervisor Declaration - Scheffer
CV - Scheffer
Supervisor Declaration - Smith
Declaration - Scheffer

Sincerely,

Franklin Weber
HREC Coordinator
Health Research Ethics Committee 1

Investigator Responsibilities

Protection of Human Research Participants

Some of the responsibilities investigators have when conducting research involving human participants are listed below:

1.Conducting the Research. You are responsible for making sure that the research is conducted according to the HREC approved research protocol. You are also responsible for the actions of all your co-investigators and research staff involved with this research.

2.Participant Enrolment. You may not recruit or enrol participants prior to the HREC approval date or after the expiration date of HREC approval. All recruitment materials for any form of media must be approved by the HREC prior to their use. If you need to recruit more participants than was noted in your HREC approval letter, you must submit an amendment requesting an increase in the number of participants.

3.Informed Consent. You are responsible for obtaining and documenting effective informed consent using **only** the HREC-approved consent documents, and for ensuring that no human participants are involved in research prior to obtaining their informed consent. Please give all participants copies of the signed informed consent documents. Keep the originals in your secured research files for at least fifteen (15) years.

4.Continuing Review. The HREC must review and approve all HREC-approved research protocols at intervals appropriate to the degree of risk but not less than once per year. There is **no grace period.** Prior to the date on which the HREC approval of the research expires, **it is your responsibility to submit the continuing review report in a timely fashion to ensure a lapse in HREC approval does not occur.** If HREC approval of your research lapses, you must stop new participant enrolment, and contact the HREC office immediately.

5.Amendments and Changes. If you wish to amend or change any aspect of your research (such as research design, interventions or procedures, number of participants, participant population, informed consent document, instruments, surveys or recruiting material), you must submit the amendment to the HREC for review using the current Amendment Form. You **may not initiate** any amendments or changes to your research without first obtaining written HREC review and approval. The **only exception** is when it is necessary to eliminate apparent immediate hazards to participants and the HREC should be immediately informed of this necessity.

6.Adverse or Unanticipated Events. Any serious adverse events, participant complaints, and all unanticipated problems that involve risks to participants or others, as well as any research-related injuries, occurring at this institution or at other performance sites must be reported to the HREC within **five (5) days** of discovery of the incident. You must also report any instances of serious or continuing problems, or non-compliance with the HRECs requirements for protecting human research participants. The only exception to this policy is that the death of a research participant must be reported in accordance with the Stellenbosch Universtiy Health Research Ethics Committee Standard Operating Procedures www.sun025.sun.ac.za/portal /page/portal/Health_Sciences/English/Centres%20and%20Institutions/Research_Development_Support/Ethics/Application_package All reportable events should be submitted to the HREC using the Serious Adverse Event Report Form.

7.Research Record Keeping. You must keep the following research-related records, at a minimum, in a secure location for a minimum of fifteen years: the HREC approved research protocol and all amendments; all informed consent documents; recruiting materials; continuing review reports; adverse or unanticipated events; and all correspondence from the HREC

8.Reports to the MCC and Sponsor. When you submit the required annual report to the MCC or you submit required reports to your sponsor, you must provide a copy of that report to the HREC. You may submit the report at the time of continuing HREC review.

9.Provision of Emergency Medical Care. When a physician provides emergency medical care to a participant without prior HREC review and approval, to the extent permitted by law, such activities will not be recognised as research nor will the data obtained by any such activities should it be used in support of research.

10.Final reports. When you have completed (no further participant enrolment, interactions, interventions or data analysis) or stopped work on your research, you must submit a Final Report to the HREC.

11.On-Site Evaluations, MCC Inspections, or Audits. If you are notified that your research will be reviewed or audited by the MCC, the sponsor, any other external agency or any internal group, you must inform the HREC immediately of the impending audit/evaluation.

Appendix D

Letter of Consent

Letter of Consent

Quantitative Hydration Sensor Development: Validation and Testing Protocol

Sub-investigators Cobus Visser & Eduard Kieser

Co-investigator Dr. M.M. Blanckenberg

Co-supervisor Prof. J. Smith

Chief Investigator / Supervisor Prof. C. Scheffer

Address Department of Mechanical and Mechatronic Engineering
Room 616
Corner of Banghoek and Jounert Str
Stellenbosch
7600
Office: 021 808 3613 - Cell: 076 907 9121 / 076 459 6484
cobusmetnc@gmail.com
ekieser@sun.ac.za
cscheffer@sun.ac.za

You are hereby invited to partake in a study to evaluate and asses the hydration status of a person subjected to dehydration. This study is completely voluntary and participants may withdraw from the study at any given time. This document highlights the testing apparatuses that will be used to measure the hydration state of the human body. It is of utmost importance that this document is read fully and that the participant fully understand what is expected of him/her. If any questions remain unanswered feel free to contact the investigators of this study. This study has been approved by the Health Research Ethics Committee of Stellenbosch and will thus be conducted in such a manner as to uphold the regulation and rules set out by them. The study will also be in accordance with the international declaration of Helsinki's ethical guidelines and principles.

The Research Study - What is it about?

Though dehydration can be experienced by all ages it has been found to have a larger detrimental affect on children [1] [2]. So much as one out of five children die as a result of dehydration, weakened immunity and malnutrition associated with diarrhoea in the world[3]. It is the aim of this project to develop measuring devices that can be used by the general populous to asses dehydration in infants as to negate possible fatality due to dehydration.

It is the purpose of this study to test and validate the sensors developed by the investigators on dehydrated subjects as to asses the hydration status of said subjects. Data collection on the effects of dehydration on a human will also make part of this project. Participants willing to participate in this study have to be older than 21 years and be healthy with no known physiological, anatomical or physical handicap or disorder. Participant who have any illness, disease or disorder will not be taken into account for this study

The study will be conducted at the Stellenbosch Coetzenburg Gym under the watchful eye of a medical practitioner. Ten to twenty people will be recruited to undergo the study (50% Men and 50% Women).

Testing Devices and Implementation

Bioelectrical Impedance Analyses Device The study will consist of the measuring of the body with up to six different devices. The first sensor will measure the impedance(electrical characteristic) of the body via a low electrical current. This is to determine the composition of the body with respect to fat-free-mass, intracellular water and extracellular water and total body

[1] Overview if Dehydration, Feb 2013, Interview, Prof. J. Smith
[2] www.pitt.edu/ super4/36011–37001/36251.ppt
[3] www.unicef.org/health/index_51412

water. This will be done by placing several electrodes over the persons body and inducing a variable frequency current through it and then measuring the resulting current dynamics or voltage.

Optical Spectrometry Device The second device uses optical spectrometry (the affect different mediums have on light through their absorption, reflecting and scattering abilities) to evaluate the water content of the skin and hopefully also the water content of blood plasma. This device will shine a certain wavelength of light (wavelength can vary from the visible spectrum up to the far infra-red spectrum) onto the skin and measure the scattering, reflectance and absorption of the light particles and from the calculated result give an indication of overall hydration.

Stratum corneum hydration probe The third device measures the water content of the stratum corneum (uppermost flaky region of the skin). This device can implement several techniques to achieve this. These techniques are:

Capacitance The device is comprised of two electrodes placed upon the skin. The device will generate a voltage over the electrodes and depending on the electrical characteristics of the stratum corneum the capacitance will change with respect to the water content of the stratum corneum.

Impedance Two electrodes will be placed upon the skin and a current will be induced through the two electrodes. The resulting voltage will be used to identify the impedance of the stratum corneum.

Optical Refraction A probe with stripped optical fibres will be placed upon the stratum corneum. The optic fibre will be excited with light and the output will be measured. Depending on the water content of the skin the light may reflect or refract at the boundary of the fibre and the stratum corneum which in turn will affect the output.

Capillary refill time monitoring This device works on the principle of capillary refill (blood reperfusion in an area of skin recently subjected to pressure). CRT is a common method used in practice to asses dehydration. The following describes the implementation of the device.

Step 1. Place the device on the back of the hand and press a button to indicate that the camera should take a picture to get the baseline skin colour.

Step 2. Push the camera down firmly while using the time and pressure read out on the device to ensure that the appropriate amount of pressure is applied for the correct time.

Step 3. Pull the camera back or allow the spring-loaded mechanism to reposition the camera sensor, where the camera will capture a frame every few milliseconds for a predetermined time. The onboard electronics will then capture the data for later analysis. The skin temperature at the measuring site will also be taken right before the CRT test since skin surface temperature affects CRT.

Optic skin turgor test The skin turgor test involves pinching the skin and evaluating the time it takes to reside back to it's original position. The test will be conducted with one of the devices to develop a quantitative measurement of dehydration. The device consists of a camera that will collect data on the dynamics of the skin after it has been pinched.

Temperature profile A hand held thermal camera will be used to record the subject's temperature profile. For the test the subject will stand up straight and a thermal image will be taken from both the front and back.

All of these devices are non-invasive and will therefore not penetrate the skin or invade any orifice. Subjects however will have to be weighed during the study and several small samples of blood (1 sample = 5mL of blood) will have to be taken by a medical practitioner. A total of six blood samples will be taken, one per day of the study . After dehydration tests are done participants will receive a light meal with Energizer or Lucozade to rehydrate and replenish the subject.

Why you?

The concept of measuring and assessing dehydration is laborious and seriously misunderstood. So far the golden rule to define a quantitative method for assessing dehydration has eluded the most brilliant of minds. It is thus necessary to form an accurate baseline of normal hydration and dehydration from which comparisons can be made. In order to form a baseline numerous tests have to be done that includes a diverse range of people. This is however not achievable due to limited time, resources and funding. It is because of this reason that healthy volunteers are needed to form the first accurate hydration sensor baseline.

What is your responsibility?

Volunteers will be asked to attend two phases of testing each phase will be 3 days long separated by a weekend. It is expected that in the first phase volunteers drink 3L of water a day between certain time intervals to achieve

a normal hydration state. This will repeated for 3 days where measurements will be taken each morning. Upon phase two volunteers will be subjected to strenuous exercise to induce dehydration. Volunteers will exercise for 50 minutes followed by a 10 minute break followed by measurements. This will be repeat three times a day for three days. Upon the completion of the day's activities the participants will have to be rehydrated and their electrolytes replenished. The participant will thus receive a light meal and Energizer or Lucozade. **NO** alcohol or caffeine may be consumed during this study as this can perturb the measurements taken and warp the baseline compromising the entire study. Notice should be given to the investigators if a participant has become ill or have contracted a disease or have succumbed to injury.

How will you benefit from this study?

Volunteers that participate **AND** complete the study will be paid. Also participants will be treated to a light meal and drink after the testing in phase two. The study will not cost you anything.

Volunteers will also help shape the initial stages to assessing and evaluating dehydration quantitatively via an apparatus. This will benefit infants, geriatric persons and most likely athletes and/or sports enthusiasts.

Is there any risk involved?

Dehydration As mentioned acute dehydration is possible. It is thus decided that volunteers will only be dehydrated as far as 4% loss of body mass. This falls under the threshold of 5% which is considered moderate dehydration [4] [5]. A Physician and/or paramedic will be present during the course of testing to ensure that no long term damage comes to volunteers due to dehydration.

Electrocution There will be no risk present with the electronic devices as measures will be taken to limit the output of the device. It is discussed in several literature sources that current is the leading factor in electrocution [6] [7] [8] Literature argues that at a current as low as 1mA the subject can experience a sensation and at 17mA could cause death [9]. In this project the current will be limited far below the danger threshold of electrocution ($<$1mA, one thousandth of an ampere) by means of a current limiter in the device to ensure current is cut off even in the presence of a low resistance brought on by water, sweat

[4] Overview of Dehydration, Feb 2013, Interview, Prof. J. Smith
[5] www.waterbenefitshealth.com/dehydration–symptoms
[6] W.R. Lee, "Death by electric shock", vol. 113, no. 1, 1966
[7] http://www.osha.gov/SLTC/etools/construction/electrical_incidents/eleccurrent.html
[8] http://www.electricityforum.com/danger–of–electricity.html
[9] http://www.osha.gov/SLTC/etools/construction/electrical_incidents/eleccurrent.html

etc. The UL26041-1 standard limits patient connected leakage current to 50 μA (fifty millionth of an ampere). The device's induced current will thus fall under this current threshold. As an added safety measure the created devices will not be powered by a wall socket, but by rechargeable batteries similar to that used by cellphones or small laptops. One can thus expect that the risk associated with handling a cellphone and a small laptop will be equivalent to the risk of handling the proposed device.

Light intensity The optical spectrometry and stratum corneum probe might implement several light diodes that will have no associated risk. The intensity of the LED's will be limited so that it falls far below the MPE (Maximum Permissible Exposure) of the skin so that no harm will befall the subject. Light sources that will be used will be similar to that of a television remote transmitter or the light sources found on a television.

Infection One of the markers of dehydration that will be measured is the osmolarity of the subject's blood plasma. This method is invasive and will thus pose a light risk of infection. A professional medical practitioner will thus be appointed to draw the blood eliminating any risk caused by inexperience.

Injury due to Exercise Subjects will be subjected to exercise which requires rigorous movement. In the event that an accident happens which causes injury to the subject medical personnel will be available to help.

Exposure to toxic materials All components or materials used in this study will consist of non-toxic materials.

Am I obligated to complete the entire study?

At any time the participant may withdraw from the study. Take note, that if this is done the entirety of the participants compensation will be forfeit, otherwise you will not be affected negatively in any way.

Who will have access to the collected information?

All data and/or information collected from the participant will be handled as confidential. No third party entity will have access to the collected information and will thus only be distributed between the principle investigators and sub-investigators. When the collected data is published participants will remain anonymous.

Miscellaneous

1. If any questions are left unanswered feel free to contact any of the two investigators (Contact details appear on the title page.)

2. Please refer all complaints and/or concerns to the Commitee for Human Reseach at 021–938 9207.

Form of Consent

Declaration by Participant

I (the applicant) ..... hereby agrees and acknowledges the following with the placement of my signature:
I declare that:

1. I have read or have been read to the contents of this document and agree to all information and/or condition given therein.
2. Ample time has been given to me to ask and/or question the information and/or conditions in this document.
3. All questions that were posed by myself have been answered and I fully comprehend the entirety of this study
4. I understand the risk involved in this study.
5. I understand that at any given time I may withdraw from the study and forfeit compensation.
6. I acknowledged that I am a volunteer participating in this study out of free will and have not been forced to do so.
7. I understand that if certain events occur, due to my actions, that jeopardises my safety and the safety of others that I may be asked to leave the study and forfeit compensation.
8. I understand that if certain events occur, due to my actions, that jeopardises the integrity of the study that I may be asked to leave and forfeit compensation.
9. I understand that I will be subjected to measurements made by experimental devices.
10. I understand that blood samples will be drawn from me for the purpose of this study.

Signed at ..... on 2013

Signature of Participant Signature of Witness

....

Form of Consent

Declaration by Investigator

I, (the investigator)....., hereby declare that:

1. I have fully explained the information in this document to .....
2. I have informed the applicant to the best of my abilities.
3. I have encouraged the applicant to ask about and/or question the risks involved in this study.
4. I have encouraged the applicant to ask about and/or question the information and conditions set out in this document.
5. That I have not forced the applicant to volunteer for the study.

Signed at ..... on 2013

Signature of Investigator Signature of Witness

....

Appendix E

Datasheets

chipKIT™ Uno32™ Board Reference Manual

Revision: October 25, 2011
Note: This document applies to REV B of the board.

DIGILENT®
www.digilentinc.com
1300 NE Henley Court, Suite 3
Pullman, WA 99163
(509) 334 6306 Voice | (509) 334 6300 Fax

Overview

The chipKIT Uno32 is based on the popular Arduino™ open-source hardware prototyping platform and adds the performance of the Microchip PIC32 microcontroller.

The Uno32 is the same form factor as the Arduino Uno board and is compatible with Arduino shields. It features a USB serial port interface for connection to the IDE and can be powered via USB or an external power supply.

The Uno32 board takes advantage of the powerful PIC32MX320F128 microcontroller. This microcontroller features a 32-bit MIPS processor core running at 80Mhz, 128K of flash program memory and 16K of SRAM data memory.

The Uno32 can be programmed using the Multi-Platform Integrated Development Environment (MPIDE), an environment based on the original Arduino IDE modified to support PIC32. It contains everything needed to start developing embedded applications.

In addition, the Uno32 is fully compatible with the advanced Microchip MPLAB® IDE and the PICKit3 in-system programmer/debugger.

The Uno32 is easy to use and suitable for both beginners and advanced users experimenting with electronics and embedded control systems.

The Uno32 provides 42 I/O pins that support a number of peripheral functions, such as UART, SPI, and I^2C ports and pulse width modulated outputs. Twelve of the I/O pins can be used as analog inputs or as digital inputs and outputs.

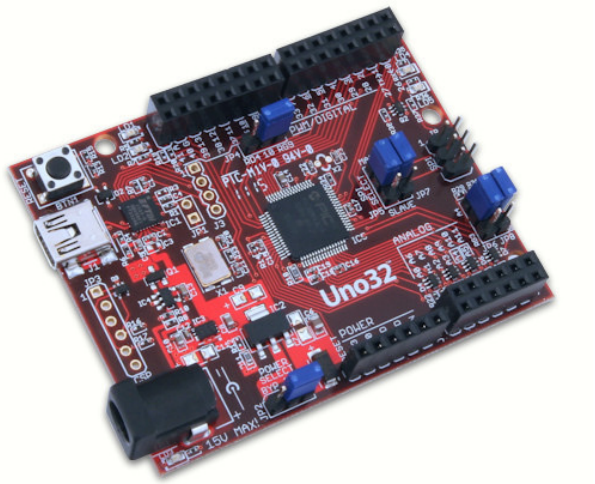

Features include:

- Microchip® PIC32MX320F128H microcontroller (80 Mhz 32-bit MIPS, 128K Flash, 16K SRAM)
- compatible with many existing Arduino code samples and other resources
- Arduino Uno form factor
- compatible with many Arduino shields
- 42 available I/O pins
- two user LEDs
- PC connection uses a USB A > mini B cable (not included)
- 12 analog inputs
- 3.3V operating voltage
- 80Mhz operating frequency
- 75mA typical operating current
- 7V to 15V input voltage (recommended)
- 20V input voltage (maximum)
- 0V to 3.3V analog input voltage range
- +/-18mA DC current per pin

chipKIT™ WiFi Shield Reference Manual

Revision: February 7, 2013
Note: This document applies to REV C of the board.

DIGILENT®
www.digilentinc.com
1300 NE Henley Court, Suite 3
Pullman, WA 99163
(509) 334 6306 Voice | (509) 334 6300 Fax

Overview

The chipKIT™ WiFi Shield is an interface board designed for use with Digilent's chipKIT line of microcontroller boards such as the Uno32™, uC32™, or Max32™. The chipKIT line is a family of microcontroller boards based on the high performance Microchip PIC32 family of microcontrollers.

The chipKIT WiFi Shield provides chipKIT microcontroller boards the ability to connect to and communicate with IEEE 802.11 compatible wireless networks.

The WiFi Shield also provides a micro-SD card connector for use with micro-SD flash memory cards. The chipKIT MPIDE SD library can be used to read/write files stored on the micro-SD card.

The WiFi Shield is intended for use with the Digilent network libraries, DNETcK and DWIFIcK, available for free download from the Digilent web site. These libraries make use of and include a custom version of the Microchip Applications Library licensed from Microchip.

Early versions of the WiFi Shield use the Microchip MRF24WB0MA WiFi module. Later versions use the improved MRF24WG0MA WiFi module.

Features include:

- IEEE 802.11b/g-compliant RF transceiver
- serialized unique MAC address
- data rates up to 11Mbps for 802.11b and 54Mbps for 802.11g possible
- WEP, WPA-PSK, WPA2-PSK security
- integrated PCB antenna
- radio regulation certification for the United States (FCC), Canada (IC), and Europe (ETSI)
- micro SD card connector
- four user accessible LEDs

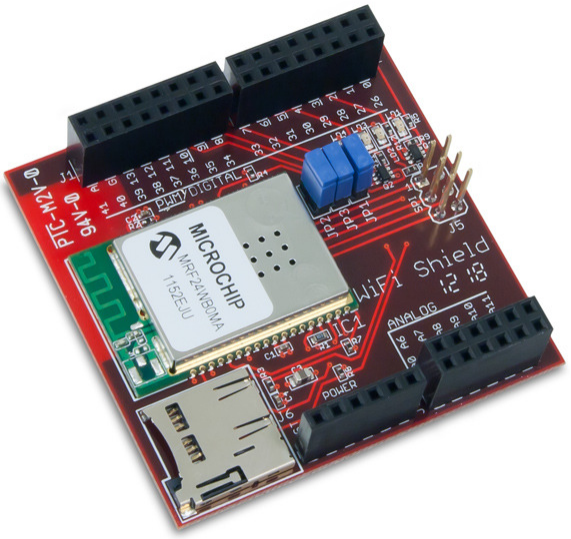

chipKIT WiFi Shield with MRF24WB0MA WiFi Module

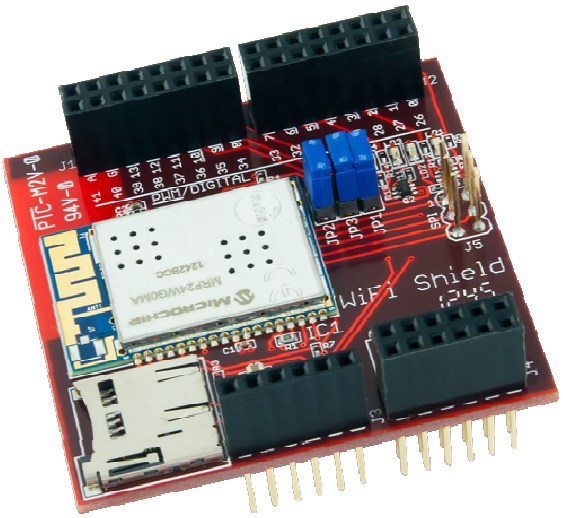

chipKIT WiFi Shield with MRF24WG0MA WiFi Module

CMOS, 125 MHz Complete DDS Synthesizer

AD9850

FEATURES

125 MHz Clock Rate
On-Chip High Performance DAC and High Speed Comparator
DAC SFDR > 50 dB @ 40 MHz A_{OUT}
32-Bit Frequency Tuning Word
Simplified Control Interface: Parallel Byte or Serial Loading Format
Phase Modulation Capability
3.3 V or 5 V Single-Supply Operation
Low Power: 380 mW @ 125 MHz (5 V)
155 mW @ 110 MHz (3.3 V)
Power-Down Function
Ultrasmall 28-Lead SSOP Packaging

APPLICATIONS

Frequency/Phase—Agile Sine Wave Synthesis
Clock Recovery and Locking Circuitry for Digital Communications
Digitally Controlled ADC Encode Generator
Agile Local Oscillator Applications

FUNCTIONAL BLOCK DIAGRAM

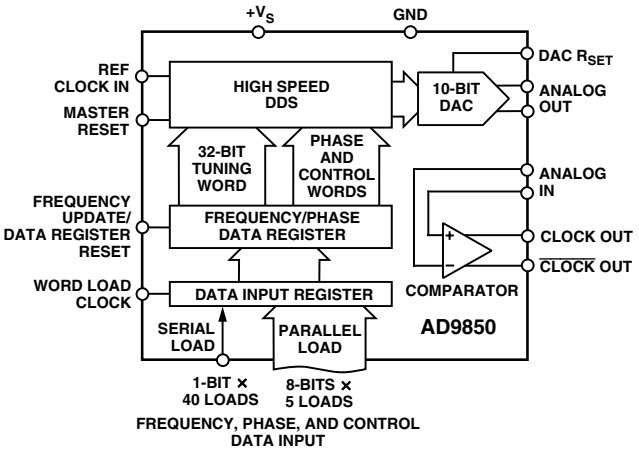

GENERAL DESCRIPTION

The AD9850 is a highly integrated device that uses advanced DDS technology coupled with an internal high speed, high performance D/A converter and comparator to form a complete, digitally programmable frequency synthesizer and clock generator function. When referenced to an accurate clock source, the AD9850 generates a spectrally pure, frequency/phase programmable, analog output sine wave. This sine wave can be used directly as a frequency source, or it can be converted to a square wave for agile-clock generator applications. The AD9850's innovative high speed DDS core provides a 32-bit frequency tuning word, which results in an output tuning resolution of 0.0291 Hz for a 125 MHz reference clock input. The AD9850's circuit architecture allows the generation of output frequencies of up to one-half the reference clock frequency (or 62.5 MHz), and the output frequency can be digitally changed (asynchronously) at a rate of up to 23 million new frequencies per second. The device also provides five bits of digitally controlled phase modulation, which enables phase shifting of its output in increments of 180°, 90°, 45°, 22.5°, 11.25°, and any combination thereof. The AD9850 also contains a high speed comparator that can be configured to accept the (externally) filtered output of the DAC to generate a low jitter square wave output. This facilitates the device's use as an agile clock generator function.

The frequency tuning, control, and phase modulation words are loaded into the AD9850 via a parallel byte or serial loading format. The parallel load format consists of five iterative loads of an 8-bit control word (byte). The first byte controls phase modulation, power-down enable, and loading format; Bytes 2 to 5 comprise the 32-bit frequency tuning word. Serial loading is accomplished via a 40-bit serial data stream on a single pin. The AD9850 Complete DDS uses advanced CMOS technology to provide this breakthrough level of functionality and performance on just 155 mW of power dissipation (3.3 V supply).

The AD9850 is available in a space-saving 28-lead SSOP, surface-mount package. It is specified to operate over the extended industrial temperature range of –40°C to +85°C.

REV. H

One Technology Way, P.O. Box 9106, Norwood, MA 02062-9106, U.S.A.
Tel: 781/329-4700 www.analog.com
Fax: 781/326-8703

ROITHNER LASERTECHNIK GmbH
WIEDNER HAUPTSTRASSE 76 1040 VIENNA AUSTRIA
TEL. +43 1 586 52 43 -0, FAX. -44, OFFICE@ROITHNER-LASER.COM

IPD14-12-5T

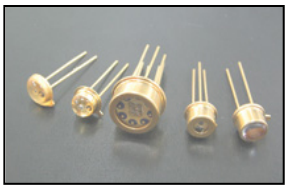

TECHNICAL DATA

Silicone PD, TO package

IPD14-12-5T is an InGaAs PIN-photodiode containing a large chip with 0.35mm² active area, mounted on a TO-18 stem and hermetical sealed by metal can with flat glass window.

Specifications

- Spectral Responsivity: 1000-1600 nm
- Active Area: 0,35 x 0,35 mm
- Package: TO-18
- Lens: Flat window glass

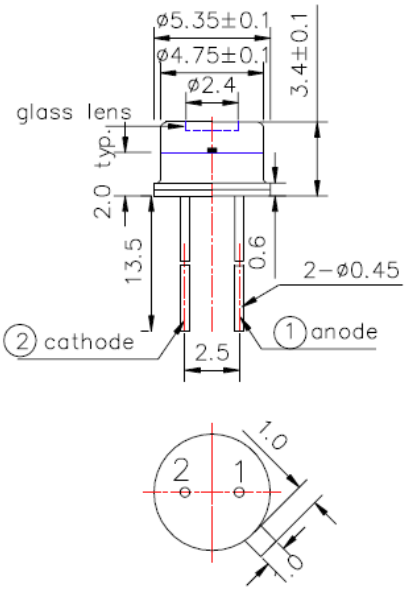

(Unit: mm)

Absolute Maximum Ratings (T_A=25°C)

Item	Symbol	Value	Unit
Reverse Breakdown Voltage	$V_{(BR)R}$	10	V
Operating Temperature	T_{opr}	-25 … +90	°C
Storage Temperature	T_{stg}	-30 … +100	°C
Soldering Temperature *[1]	T_{sol}	260	°C

*[1] must be completed within 3 seconds.

Electro-Optical Characteristics

Item	Symbol	Condition	Min.	Typ.	Max.	Unit
Photo Responsivity	R_E	V_R=0V, $\lambda_{P=}$1450nm	-	0,9	-	A/W
Photo Current	I_L	V_R=0V, $\lambda_{P=}$1450nm	10	14	-	µA
Dark Current	I_D	V_R=1V	-	-	100	nA
Open Circuit Voltage	V_{OC}	V_R=10V, L=1000Lx	-	410	-	mV
Spectral Responsivity (Peak)	λ_P		1000		1600	nm
Half Angle of Sensitivity	$\Theta_{1/2}$	V_R=0V		±40	-	deg
Total Capacitance	C_T	V_R=1V, f=1MHz	-	20	-	pF
Rise Time (10-90%)	t_r	R_L=1KΩ, V_R=1V	-	10	-	ns
Fall Time (10-90%)	t_f		-	5	-	ns

Note: The above specifications are for reference purpose only and subjected to change without prior notice.

ROITHNER LASERTECHNIK GmbH
WIEDNER HAUPTSTRASSE 76 1040 VIENNA AUSTRIA
TEL. +43 1 586 52 43 -0, FAX. -44, OFFICE@ROITHNER-LASER.COM

LED1300-series

TECHNICAL DATA

Infrared LED InGaAsP

LED1300-series are InGaAsP LEDs mounted on a lead frame and encapsulated in various types of epoxy lens, which offers different design settings.
On forward bias, it emits a high power radiation of typical 4.5 mW at a peak wavelength at 1300 nm.

Specifications

- Structure: InGaAsP
- Peak Wavelength: typ. 1300 nm
- Optical Ouput Power: typ. 4.5 mW
- Resin Material: Epoxy resin
- Solder: Lead free

Absolute Maximum Ratings (T_a=25°C)

Type	Symbol	Value	Unit
Power Dissipation	P_D	140	mW
Forward Current	I_F	100	mA
Pulse Forward Current	I_{FP}	1000	mA
Reverse Voltage	V_R	5	V
Operating Temperature	T_{OP}	-40 … +85	°C
Storage Temperature	T_{STG}	-40 … +100	°C
Soldering Temperature (for 5 sec.)	T_{SOL}	265	°C

Electro-Optical Characteristics (T_a=25°C)

Item	Symbol	Condition	Min.	Typ.	Max.	Unit
Forward Voltage	V_F	I_F = 50 mA	-	1.0	1.5	V
Reverse Current	I_R	V_R = 5 V	-	-	10	µA
Radiated Power	P_O	I_F = 50 mA	2.5	4.5	-	mW
Peak Wavelength	λ_P	I_F = 50 mA	1250	1300	1350	nm
Half Width	$\Delta\lambda$	I_F = 50 mA	-	80	-	nm
Rise Time	t_r	I_F = 50 mA	-	10	-	ns
Fall Time	t_f	I_F = 50 mA	-	10	-	ns

ROITHNER LASERTECHNIK
Wiedner Hauptstraße 76, A-1040 Vienna, Austria
Tel.: ++43 1 586 52 43-0, Fax -44, office@roithner-laser.com

LED - Lamp

ELD-1480-525

22.10.2008 rev. 01

Radiation	Type	Technology	Case
Infrared	MQW	InGaAs/InP	5 mm plastic lens

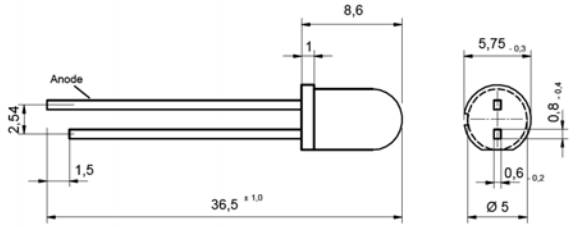

Description

High-power, high-speed infrared LED in standard 5 mm package, housing without standoff leads

Note: Special packages with standoff available on request

Applications

Optical communications, safety equipment, automation

Maximum Ratings

T_{amb} = 25℃, unless otherwise specified

Parameter	Test conditions	Symbol	Value	Unit
Forward current (DC)		I_F	100	mA
Peak forward current	($t_P \leq 50$ µs, $t_P/T = 1/2$)	I_{FM}	200	mA
Power dissipation		P_D	150	mW
Operating temperature range		T_{amb}	-20 to +80	℃
Storage temperature range		T_{stg}	-55 to +100	℃
Soldering temperature	t ≤ 5 s, 3 mm from case	T_{sd}	260	℃

Optical and Electrical Characteristics

T_{amb} = 25℃, unless otherwise specified

Parameter	Test conditions	Symbol	Min	Typ	Max	Unit
Forward voltage	I_F = 20 mA	V_F		0,80		V
Forward voltage*	I_F = 100 mA	V_F		1,0		V
Reverse voltage	I_R = 100 µA	V_R	5			V
Radiant power	I_F = 20 mA	Φ_e		1,8		mW
Radiant power*	I_F = 100 mA	Φ_e		6,5		mW
Peak wavelength	I_F = 100 mA	λ_p		1460		nm
Spectral bandwidth at 50%	I_F = 100 mA	$\Delta\lambda_{0.5}$		150		nm
Viewing angle	I_F = 100 mA	φ		20		deg.
Switching time	I_F = 100 mA	t_r, t_f		40		ns

*for information only

List of References

[1] T. Takeo and H. Hattori, "Skin hydration state estimation using a fiber-optic refractometer," *Applied optics*, vol. 33, no. 19, pp. 4267–4272, 1994.

[2] (2012) Brighterlooks: How it works. Accessed: 2014-12-03. [Online]. Available: http://www.brighterlooks.com/how-it-works/

[3] R. Nachabé, B. H. Hendriks, M. van der Voort, A. E. Desjardins, and H. J. Sterenborg, "Estimation of biological chromophores using diffuse optical spectroscopy: benefit of extending the uv-vis wavelength range to include 1000 to 1600 nm," *Biomedical optics express*, vol. 1, no. 5, pp. 1432–1442, 2010.

[4] J. Smith, "An Overview of Dehydration," Feb. 2013, interview.

[5] P. R. Earl. (2009, Dec.) Dehydration. Accessed: 2013-07-29. [Online]. Available: http://www.pitt.edu/~super4/36011-37001/36251.ppt

[6] Unicef. (2012, May) Diarrhoea: Why children are still dying and what can be done. Accessed: 2013-07-29. [Online]. Available: http://www.unicef.org/health/index_51412.html

[7] L. E. Armstrong, "Assessing hydration status: the elusive gold standard," *Journal of the American College of Nutrition*, vol. 26, no. sup5, pp. 575S–584S, 2007.

[8] S. H. Hamed, B. Altrabsheh, T. Assa'd, S. Jaradat, M. Alshra'ah, A. Al-jamal, H. S. Alkhatib, and A.-M. Almalty, "Construction, in vitro and in vivo evaluation of an in-house conductance meter for measurement of skin hydration." *Medical engineering & physics*, vol. 34, no. 10, pp. 1471–6, Dec. 2012.

[9] Ø. G. Martinsen, S. Grimnes, and E. Haug, "Measuring depth depends on frequency in electrical skin impedance measurements," *Skin Research and Technology*, vol. 5, no. 3, pp. 179–181, 1999.

[10] S. N. Cheuvront, R. W. Kenefick, N. Charkoudian, and M. N. Sawka, "Physiologic basis for understanding quantitative dehydration assess-

ment," *The American journal of clinical nutrition*, vol. 97, no. 3, pp. 455–462, 2013.

[11] R. W. Kenefick, S. N. Cheuvront, L. Leon, and K. K. O'Brien, "Dehydration and rehydration," DTIC Document, Tech. Rep., 2012.

[12] S. I. Fox, *Fundamentals of human physiology*. McGraw-Hill, 2009.

[13] N. Charkoudian, "Mechanisms and modifiers of reflex induced cutaneous," *J Appl Physiol*, vol. 110, no. 5, pp. 1264–1270, 2011.

[14] S. Shirreffs, "Markers of hydration status," *European journal of clinical nutrition*, vol. 57, pp. S6–S9, 2003.

[15] L. Röthlingshöfer, M. Ulbrich, S. Hahne, and S. Leonhardt, "Monitoring change of body fluid during physical exercise using bioimpedance spectroscopy and finite element simulations," *Journal of Electrical Bioimpedance*, vol. 2, no. 1, pp. 79–85, 2011.

[16] M. Y. Jaffrin and H. Morel, "Body fluid volumes measurements by impedance: A review of bioimpedance spectroscopy (bis) and bioimpedance analysis (bia) methods," *Medical engineering & physics*, vol. 30, no. 10, pp. 1257–1269, 2008.

[17] U. G. Kyle, I. Bosaeus, A. D. De Lorenzo, P. Deurenberg, M. Elia, J. M. Gómez, B. L. Heitmann, L. Kent-Smith, J.-C. Melchior, M. Pirlich *et al.*, "Bioelectrical impedance analysis part i: review of principles and methods," *Clinical Nutrition*, vol. 23, no. 5, pp. 1226–1243, 2004.

[18] J. Krider. (2006, Feb.) Bioelectrical impedance - bia. Accessed: 2013-07-23. [Online]. Available: http://www.formulamedical.com/formulaforlife/measurement&diaries/BIA

[19] ImpediMed. (2012) Fluid Status / Body Composition. Accessed: 2013-07-23. [Online]. Available: http://www.impedimed.com/medical-applications/fluid-status-body-composition

[20] H. Tagami, K. Kikuchi, and K. O'goshi, *Electrical Properties of Newborn Skin*, ser. Neonatal Skin: Strucure and Function. CRC Press, Jan. 2003, ch. 9, pp. 179–200.

[21] M. Stöppler. (2013, May) Dehydration: What are the signs and symptoms of dehydration? Accessed: 2013-07-25. [Online]. Available: http://www.medicinenet.com/dehydration/page3.htm#what_are_the_signs_and_symptoms_of_dehydration

[22] MayoClinic. (2011, Jan.) Dehydration: Symptoms. Accessed: 2013-07-25. [Online]. Available: http://www.mayoclinic.com/health/dehydration/DS00561/DSECTION=symptoms

[23] U. Birgersson, "Electrical impedance of human skin and tissue alterations: Mathematical modeling and measurements," 2012.

[24] M. Friebel, K. Do, A. Hahn, G. Mu *et al.*, "Optical properties of circulating human blood in the wavelength range 400–2500 nm," *Journal of biomedical optics*, vol. 4, no. 1, pp. 36–46, 1999.

[25] A. Bashkatov, E. Genina, V. Kochubey, and V. Tuchin, "Optical properties of human skin, subcutaneous and mucous tissues in the wavelength range from 400 to 2000 nm," *Journal of Physics D: Applied Physics*, vol. 38, no. 15, p. 2543, 2005.

[26] R. Shaw and H. Mantsch, "Infrared spectroscopy in clinical and diagnostic analyses," 2000.

[27] S. N. Cheuvront, B. R. Ely, R. W. Kenefick, and M. N. Sawka, "Biological variation and diagnostic accuracy of dehydration assessment markers," *The American journal of clinical nutrition*, vol. 92, no. 3, pp. 565–573, 2010.

[28] K. P. Nielsen, L. Zhao, J. J. Stamnes, K. Stamnes, and J. Moan, "The optics of human skin: aspects important for human health," *Norw. Acad. Sci. Lett*, pp. 35–46, 2008.

[29] S. L. Jacques and S. A. Prahl. (1998) Introduction to biomedical optics. Accessed 10 October 2014. [Online]. Available: http://omlc.org/education/ece532/index.html

[30] J. Sørensen Dam, *Optical analysis of biological media-continuous wave diffuse spectroscopy*. Lund University, 2000.

[31] A. E. Karsten, "The effect of skin phototype on laser propagation through skin."

[32] T. L. Troy and S. N. Thennadil, "Optical properties of human skin in the near infrared wavelength range of 1000 to 2200 nm," *Journal of Biomedical Optics*, vol. 6, no. 2, pp. 167–176, 2001.

[33] Z. Gajinov, M. Matić, S. Prćić, and V. Đuran, "Optical properties of the human skin/optičke osobine ljudske kože," *Serbian Journal of Dermatology and Venerology*, vol. 2, no. 4, pp. 131–136, 2010.

[34] A. N. Bashkatov, E. A. Genina, and V. V. Tuchin, "Optical properties of skin, subcutaneous, and muscle tissues: a review," *Journal of Innovative Optical Health Sciences*, vol. 4, no. 01, pp. 9–38, 2011.

[35] Roithner lasertechnik. Accessed: 2014-12-03. [Online]. Available: http://www.roithner-laser.com/index.html

[36] S. Grimnes and Ø. G. Martinsen, "Bioimpedance," *Wiley Encyclopedia of Biomedical Engineering*, 2006.

[37] K. R. Foster and H. C. Lukaski, "Whole-body impedance–what does it measure?" *The American journal of clinical nutrition*, vol. 64, no. 3, pp. 388S–396S, 1996.